

See discussions, stats, and author profiles for this publication at: <https://www.researchgate.net/publication/259892724>

Modeling Interfacial Tension in Liquid-Liquid Systems Containing Electrolytes

ARTICLE in INDUSTRIAL & ENGINEERING CHEMISTRY RESEARCH · MAY 2013

Impact Factor: 2.59 · DOI: 10.1021/ie303460c

CITATIONS

6

READS

38

2 AUTHORS, INCLUDING:



Peiming Wang

OLI Systems, Inc.

48 PUBLICATIONS 1,077 CITATIONS

SEE PROFILE

Modeling Interfacial Tension in Liquid–Liquid Systems Containing Electrolytes

Peiming Wang* and Andrzej Anderko

OLI Systems Inc., 240 Cedar Knolls Road, Suite 301, Cedar Knolls, New Jersey 07927, United States

ABSTRACT: A comprehensive model has been developed for calculating the interfacial tension (σ) in liquid–liquid systems with or without electrolyte components. The model consists of an equation for computing the interfacial tension of two-liquid-phase nonelectrolyte systems and an expression for the effect of the electrolyte concentration. The dependence of the interfacial tension on the electrolyte concentration was derived by combining the Gibbs equation with a modified Langmuir adsorption isotherm that represents the interfacial excess of the solute species. The Langmuir adsorption formalism was extended by introducing the effects of binary interactions between solute species (ions or molecules) on the interface. The equation for the interfacial tension of nonelectrolyte liquid–liquid systems was derived using a general thermodynamic framework that was empirically extended by introducing an effective interfacial area that is defined for each component and takes into account the effects of other components at the interface. The model was found to reproduce experimental data for a variety of liquid–liquid systems. In particular, the interfacial tension of ternary systems can be accurately predicted using parameters determined from only binary data. Furthermore, the interfacial tension model was coupled with a previously developed thermodynamic model to provide activity coefficients and equilibrium concentrations in coexisting liquid phases. This makes it possible to reproduce the effects of speciation and salting out or salting in. Because of the coupling of the thermodynamic model with interfacial tension calculations, the variation of σ with electrolyte concentration can be reasonably predicted even without introducing electrolyte-specific parameters in the interfacial tension model. Thus, the model can be used to estimate the electrolyte effect on σ in the absence of experimental data. With regressed model parameters, the average deviations between the calculated results and experimental data were 0.50 mN·m^{−1} for 30 binary nonelectrolyte systems, 0.88 mN·m^{−1} for 23 ternary nonelectrolyte systems, and 0.16 mN·m^{−1} for 26 systems with ionic components.

1. INTRODUCTION

Interfacial tension is one of the most important properties characterizing inhomogeneous liquid systems. Understanding the behavior of liquid–liquid interfaces is of paramount significance for the rational design of numerous processes such as those encountered in coatings and adsorption, industrial separations involving extraction, enhanced oil recovery, and emulsions and suspensions in the food and pharmaceutical industries. For example, interfacial tension is an important factor that influences the partitioning behavior of species (molecules or ions) between two liquid phases. The degree of interfacial adsorption of species is directly associated with interfacial tension. Furthermore, the properties of the liquid–liquid interface and, in particular, the value of the interfacial tension provide insight into the mechanism of distribution of species in liquid–liquid systems, which is of interest for the design of liquid–liquid extraction in separation processes. Because of their practical importance, studies of interfacial tension and interfacial chemistry have represented an area of active research over the past century. Accurate determination of interfacial tension for various liquid–liquid systems is important for gaining insight into the interfacial processes for the transfer of mass and energy across the phase boundary. Over the past several decades, a large amount of experimental interfacial tension data has been reported for various liquid–liquid systems, especially for mixtures of organic liquids and water. Interfacial tension data have also been fairly reported for systems containing electrolytes. Thus, the experimental data that are available in the literature provide a

basis for a comprehensive analysis of the factors that influence the interfacial tension in two-liquid systems involving nonelectrolyte (e.g., organic + water) and electrolyte components.

Various approaches have been reported in the literature to model the liquid–liquid interfacial tension. Most of the methods that are available for the prediction of nonelectrolyte liquid–liquid interfacial tension are based on the mutual solubility as an input variable^{1–10} because the miscibility and interfacial tension reflect the same intermolecular forces and are inherently related.^{5,11} Interfacial tension between two liquid phases has also been correlated with the surface tensions of the two coexisting liquid phases by the simple Antonow's rule¹² or through an interaction parameter that characterizes the similarity of the intermolecular forces between the two liquids.¹³ The published interfacial tension models range from applications of the thermodynamic equation of Shain and Prausnitz,¹ as exemplified by the models of Fu et al.² and Bahramian and Danesh,⁷ to those based on solution theories such as the quasilattice and regular solution approximations,^{3,9} the gradient theory,¹⁴ and the scaling theory of critical phenomena.¹⁵ Moreover, a model based on the Gibbs–Langmuir monolayer adsorption isotherm has been reported.¹⁰ There are also empirically based models^{5,12,16} that are often

Received: December 14, 2012

Revised: April 24, 2013

Accepted: April 25, 2013

Published: April 26, 2013

convenient in practical engineering calculations. Assessments and comparisons of various methods that are available for estimating interfacial tension in nonelectrolyte systems have also been reported.^{11,17,18}

In contrast to nonelectrolyte systems and also to liquid–gas surface tension, the liquid–liquid interfacial tension behavior of systems containing electrolytes is much less comprehensively understood, even though the interfaces of two immiscible electrolyte solutions have been studied for many years¹⁹ and models for the electrolyte effect on interfacial tension have been reported. The most recently published models for such systems include those of Bier et al.,²⁰ Onuki,²¹ and dos Santos and Levin.^{22,23} Because of the low dielectric constants of organic solvents, especially of oil components, ion interactions at oil–water interfaces have been assumed to be similar to those at the liquid–gas interfaces in treatments using the dielectric continuum theory.²² Indeed, the liquid–liquid interfacial tension data that are reported as a function of electrolyte concentration seem to show a trend similar to that of the liquid–gas surface tension, namely, the interfacial tension increases nearly linearly with electrolyte concentration at large ionic strengths for most of the reported systems. On the other hand, limiting behavior derived from the theory of Onsager and Samaras²⁴ for liquid–gas surfaces at low ionic strengths cannot be expected for liquid–liquid interfaces because of ion partitioning between the two phases.²⁰ Rather, a limiting behavior that scales with the square root of the ionic strength has been derived for liquid–liquid interfacial tension.^{20,21} For more concentrated electrolyte solutions, an approach that combines the thermodynamic treatment embodied in the Gibbs equation¹² with an adsorption isotherm has been proposed.^{25,26} In such an approach, the adsorption isotherm defines the interfacial concentrations of the electrolyte components. The activities required in the Gibbs equation are then determined by introducing an activity coefficient model. The applicability range of this approach is generally limited by that of the activity coefficient model. For example, the Meissner²⁷ method for predicting activity coefficients was used by Li and Lu²⁶ in their interfacial tension model, and therefore, the applicability range of the Li–Lu²⁶ model coincides with that of the Meissner model, which is generally valid up to a few molal for most electrolyte systems.²⁷ These models have been successfully applied to represent interfacial tension between an organic solvent and aqueous electrolyte solutions. It should be noted that these models do not take into account the chemical speciation in electrolyte solutions, which can be significant for highly associated systems such as sulfuric acid. For example, it is noteworthy that interfacial tension in the benzene–water–H₂SO₄ system shows a minimum as a function of acid concentration, which would be difficult to represent using the existing models without taking into account the complex speciation patterns of sulfuric acid. Also, these models neglect the presence of electrolytes and water in the organic, or second liquid, phase and assume that the activities of the organic solvent and possible metal–organic complexes are negligible in the aqueous phase.^{25,26} Such assumptions might be justified for systems in which the solvent components (i.e., water and an organic compound) show a wide miscibility gap and the organic solvent is highly hydrophobic, but might lead to unreasonable results for systems in which both liquid phases contain significant or non-negligible amounts of ionic species (e.g., ionic liquids + water) or both phases are water-dominated (e.g., aqueous two-phase systems, or ATPSs).

In a liquid–liquid system containing electrolytes, interfacial tension is determined not only by the concentrations of electrolytes, but also by the mutual solubility of the solvent components, which is often a function of temperature and pressure. Thus, liquid–liquid interfacial tension strongly depends on the equilibrium concentrations of the mixed-solvent electrolyte system. In addition, in systems with strong ion association effects, interfacial tension—like most thermophysical properties—is expected to be influenced by the concentrations of both ions and associated ion pairs. Thus, a comprehensive treatment of interfacial tension in mixed-solvent electrolyte systems requires one to take account not only the ion–solvent and ion–ion interactions that predominate in aqueous solutions, but also the solvent–solvent and ion pair–solvent interactions. This is possible only if a comprehensive, speciation-based framework is used as a thermodynamic foundation for the interfacial tension model.

The objective of this work is to develop a comprehensive, engineering-oriented model for predicting liquid–liquid interfacial tension in systems containing nonelectrolyte and electrolyte components. The model is designed to account for speciation effects, such as complexation or ion association, which can be obtained from a separate speciation-based thermodynamic model. The model developed in this study consists of two parts: (1) computation of the interfacial tension of nonelectrolyte liquid–liquid systems and (2) evaluation of the dependence of the interfacial tension on the electrolyte concentration.

2. INTERFACIAL TENSION IN NONELECTROLYTE LIQUID–LIQUID SYSTEMS

The interfacial tension model for nonelectrolyte systems is derived on the basis of a rigorous thermodynamic framework that was introduced by Shain and Prausnitz.¹ For completeness, the derivation of this framework is summarized in Appendix A. In this approach, the interfacial tension (σ) is related to the activities of a component in the bulk liquid phases ($a_i = x_i\gamma_i$) and at the interface ($x_i^{\text{int}}, \gamma_i^{\text{int}}$)

$$a_i = x_i\gamma_i = x_i^{\text{int}}\gamma_i^{\text{int}} \exp\left(-\frac{\sigma \bar{A}_i^{\text{int}}}{RT}\right) \quad (1)$$

where \bar{A}_i^{int} is the partial molar interfacial area of component i . The exponential term in eq 1 can be interpreted as a correction to the product $x_i^{\text{int}}\gamma_i^{\text{int}}$ and is necessary to account for the interfacial effects determined by \bar{A}_i^{int} . Combining eq 1 with the mole fraction constraint for the interfacial phase, that is

$$\sum_i x_i^{\text{int}} = 1$$

results in the expression

$$\sum_i \frac{x_i\gamma_i}{\gamma_i^{\text{int}}} \exp\left(\frac{\sigma \bar{A}_i^{\text{int}}}{RT}\right) = 1 \quad (2)$$

Whereas the activity coefficients of the components in the bulk liquid phases can be determined directly from the activity coefficient model,²⁸ those at the interface, γ_i^{int} , need to be evaluated separately, together with the partial molar interfacial area, \bar{A}_i^{int} .

To evaluate the activity coefficients of the components at the interface, Backes et al.⁶ assumed that the composition of the interfacial region is a point on the tie line that links the bulk phases in an N -dimensional concentration space, where N stands for the number of components in the system. The activity coefficients of the components at the interface are then calculated using the same model as for the bulk liquid phases. An alternative approach was proposed by Bahramian and Danesh,⁷ who employed lattice theory and the regular solution assumption to relate the activity coefficients of each component at the interface (γ_i^{int}) to those in the two bulk liquid phases (γ_i^α and γ_i^β)

$$\gamma_i^{\text{int}} = (\gamma_i^\alpha \gamma_i^\beta)^{1/2} \quad (3)$$

By applying eq 3 and the equilibrium condition $x_i^\alpha \gamma_i^\alpha = x_i^\beta \gamma_i^\beta$, eq 2 becomes

$$\sum_i (x_i^\alpha x_i^\beta)^{1/2} \exp\left(\frac{\sigma \overline{A}_i^{\text{int}}}{RT}\right) = 1 \quad (4)$$

where the sum in eq 4 is over all components in the system. In this study, we adopt the approximation of Bahramian and Danesh,⁷ namely, eq 4. Computation of the interfacial tension, σ , from eq 4 requires a prior determination of the partial molar interfacial area $\overline{A}_i^{\text{int}}$. Sprow and Prausnitz²⁹ estimated $\overline{A}_i^{\text{int}}$ from the partial molar volume of component i in the interfacial mixture (v_i^{int})

$$\overline{A}_i^{\text{int}} = (v_i^{\text{int}})^{2/3} (N_A)^{1/3} \quad (5)$$

where N_A is Avogadro's number. The partial molar interfacial area can also be estimated from the van der Waals area of the molecule as described by Bondi.^{30,31} The estimation of the partial molar interfacial area using eq 5 and other methods^{30,31} has been based on spherical molecules, which can be a crude assumption. The partial molar volume of a component in the interfacial phase should, in general, depend on the temperature, pressure, and composition of the two liquid phases that are adjacent to it. In view of the absence of a rigorous method for calculating the partial molar interfacial area, a mixing rule is proposed in this study for estimating $\overline{A}_i^{\text{int}}$ using eq 5. The mixing rule uses the pure-component molar volume of component i as a reasonable reference point for the partial molar volume. Then, it adds binary terms that account for the effects of other components on the partial molar volume in the mixture. The binary terms need to be weighted by the concentrations of components in the coexisting phases because the interfacial concentration is intermediate between those in the bulk phases α and β . Accordingly, the mixing rule for the interfacial molar volume of component i is expressed as

$$v_i^{\text{int}} = v_i^0 + \sum_{j \neq i} (x_j^\alpha + x_j^\beta) k_{ij} v_j^0 \quad (6)$$

where v_i^0 and v_j^0 are the molar volumes of the pure liquids i and j , respectively; x_j^α and x_j^β are the equilibrium concentrations (in mole fractions) of component j in liquid phases α and β , respectively; and k_{ij} is an adjustable parameter that can be determined from experimental interfacial tension data. Equation 6 reflects the effect of the compositions of the two coexisting liquid phases on the partial molar volume of the component at the interface. The parameter k_{ij} represents the extent of this effect. When all k_{ij} values are zero, v_i^{int} becomes

equal to the pure-component liquid volume, v_i^0 . Equation 6 remains invariant to dividing any component into two identical pseudocomponents, and therefore, it satisfies an important internal consistency check for empirical mixing rules (i.e., it avoids the so-called Michelsen–Kistenmacher syndrome³²).

By combining the equilibrium composition of the two liquid phases with the partial molar interfacial area $\overline{A}_i^{\text{int}}$ from eqs 5 and 6, the interfacial tension, σ , can be obtained by solving eq 4. It should be noted that the equilibrium concentrations in the two liquid phases, x_i^α and x_i^β , which are required for calculating the interfacial tension in eq 4, are determined here from the thermodynamic activity coefficient model.²⁸ The thermodynamic model was developed previously and has been extensively validated using experimental data on phase equilibria and other thermodynamic properties for a variety of systems including those with liquid–liquid phase splitting.^{33,34}

3. EFFECT OF ELECTROLYTE CONCENTRATION ON INTERFACIAL TENSION

3.1. Thermodynamic Treatment: The Gibbs Equation.

For a given system at constant temperature and pressure, the change with composition of the interfacial tension σ between two liquid phases, α and β , can be expressed using the Gibbs equation

$$d\sigma = - \sum_i \Gamma_i^\sigma d\mu_i \quad (7)$$

where μ_i is the chemical potential of species i and Γ_i^σ is the interfacial excess of component i ,¹² which represents the excess (a positive difference from the bulk value) or deficiency (a negative difference) of any component i , per unit area, at the interface. Γ_i^σ depends on the compositions of the two liquid phases and the interface. Equation 7 thus describes the change of interfacial free energy between two equilibrium states of a two-phase system.

Based on the theory of the Gibbs dividing interface,^{12,35} the interfacial excess can be defined on the basis of any arbitrarily chosen dividing interface in the interfacial region. Following Shain and Prausnitz,¹ a dividing interface was selected such that the interfacial excess of any solvent component is identically equal to zero, or $\sum_l \Gamma_l^\sigma d\mu_l = 0$, where the sum is over all solvent components l and N_s is the number of solvent components (miscible or immiscible). Such a definition of the dividing interface is equivalent to a reference state in which any deviation from the interfacial tension of an immiscible solvent mixture is attributed to the effect of the solute (i.e., electrolyte) concentration.

To transition from eq 7 to a practical equation that can work together with engineering-oriented Gibbs energy models for liquid–liquid equilibrium (LLE) calculations, it is necessary to consider the general LLE conditions for systems with ionic components. The liquid–liquid equilibrium criterion for such systems was discussed in a previous study.³³ Fundamentally, the chemical potentials of each neutral species i in the two coexisting phases, α and β , are equal

$$\mu_i^\alpha = \mu_i^\beta \quad (8a)$$

When the system contains electrolytes (e.g., $C_\nu A_\nu$), the liquid–liquid equilibrium condition can be defined as³³

$$\mu_{C_{\nu_c}A_{\nu_a}}^{\alpha} = \mu_{C_{\nu_c}A_{\nu_a}}^{\beta} \quad (8b)$$

where

$$\mu_{C_{\nu_c}A_{\nu_a}} = \nu_c \mu_C + \nu_a \mu_A \quad (8c)$$

Equations 8b and 8c lead to the equality of the mean activities of the electrolyte in the two liquid phases at equilibrium

$$(a_{\pm})^{\alpha} = (a_{\pm})^{\beta} \quad (8d)$$

where $a_{\pm} = (a_C^{\nu_c} a_A^{\nu_a})^{1/\nu}$ and $\nu = \nu_c + \nu_a$. Such a definition is based on the fact that only the chemical potential of an electrically neutral salt is experimentally accessible because of the electroneutrality condition for every phase. Consequently, this constraint can be applied to all cation–anion pairs when the system contains multiple ions.³³ Notwithstanding this thermodynamic relationship, it has been noted in the literature that a complete thermodynamic treatment of liquid–liquid equilibria in multicomponent electrolyte systems requires calculation of the contact potential between the two phases in equilibrium.³⁶ Specifically, the electrochemical potential of the ionic species should include an electrostatic contribution in addition to a chemical term

$$\mu_i = \mu_i^{\text{chem}} + z_i F \phi = \mu_i^0 + RT \ln a_i + z_i F \phi \quad (9)$$

where ϕ is the electrostatic potential. The contact potential can then be obtained as the difference in the electrostatic potentials of the neutral cation–anion pairs in both phases at equilibrium as represented by eq 8b results in the cancellation of the terms that contain ϕ . In fact, Haynes et al.³⁶ noted that knowledge of the interfacial electrostatic potential difference between two phases in equilibrium is not necessary for the determination of equilibrium compositions or any other thermodynamic properties of two-liquid-phase systems, but is useful for understanding the intermolecular forces acting on the charged species at the interface.

An appropriate expression for the composition dependence of the interfacial tension can then be derived by considering the fact that the chemical potential of species i , μ_i , should be the same at equilibrium in each of the two liquid phases and at the interface. Thus, for neutral species

$$\mu_N = \mu_N^{\sigma} = \mu_N^{\alpha} = \mu_N^{\beta} \quad (10a)$$

$$\mu_N = \mu_N^0 + RT \ln a_N \quad (10b)$$

$$d\mu_N = RT \, d \ln a_N \quad (10c)$$

where a_N is the activity of species N in the liquid phase, which is the same in the phases α and β . For an electrolyte $C_{\nu_c}A_{\nu_a}$

$$\mu_{C_{\nu_c}A_{\nu_a}} = \mu_{C_{\nu_c}A_{\nu_a}}^{\sigma} = \mu_{C_{\nu_c}A_{\nu_a}}^{\alpha} = \mu_{C_{\nu_c}A_{\nu_a}}^{\beta} \quad (11a)$$

$$\begin{aligned} \mu_{C_{\nu_c}A_{\nu_a}} &= \nu_c \mu_C + \nu_a \mu_A \\ &= (\nu_c \mu_C^0 + \nu_a \mu_A^0) + (\nu_c RT \ln a_C + \nu_a RT \ln a_A) \end{aligned} \quad (11b)$$

$$d\mu_{C_{\nu_c}A_{\nu_a}} = \nu_c RT \, d \ln a_C + \nu_a RT \, d \ln a_A \quad (11c)$$

where a_C and a_A are the activities of cation C and anion A , respectively, which satisfy the equilibrium criterion defined in eq 8d. In eq 11a, the electrostatic potential terms cancel. Thus,

eq 7 can be expressed to include contributions from neutral species (N) and the electrically neutral cation–anion pairs ($C_{\nu_c}A_{\nu_a}$)

$$d\sigma = - \sum_N \Gamma_N^{\sigma} d\mu_N - \sum_{C_{\nu_c}A_{\nu_a}} \Gamma_{C_{\nu_c}A_{\nu_a}}^{\sigma} d\mu_{C_{\nu_c}A_{\nu_a}} \quad (12)$$

It can be easily shown that

$$\sum_{C_{\nu_c}A_{\nu_a}} \Gamma_{C_{\nu_c}A_{\nu_a}}^{\sigma} d\mu_{C_{\nu_c}A_{\nu_a}} = \sum_I \Gamma_I^{\sigma} d\mu_I^{\text{chem}} \quad (13a)$$

where I denotes the constituent ions and

$$d\mu_I^{\text{chem}} = RT \, d \ln a_I \quad (13b)$$

$$\Gamma_I^{\sigma} = \sum_{\nu_I} \nu_I \Gamma_{C_{\nu_c}A_{\nu_a}}^{\sigma}(I) \quad (13c)$$

In eq 13b, the superscript chem in $d\mu_I^{\text{chem}}$ is used to distinguish the chemical contribution to the chemical potential from the complete electrochemical potential, $d\mu_I$, which includes the electrostatic term for ion I that was canceled in $d\mu_{C_{\nu_c}A_{\nu_a}}$. The sum in eq 13c includes all electrolytes $C_{\nu_c}A_{\nu_a}$ that contain the ion I , and ν_I is the number of ions I (cation or anion) in $C_{\nu_c}A_{\nu_a}$.

Substituting eqs 10c and 11c into eq 12 and applying eqs 13a–13c yields

$$d\sigma = -RT \sum_i \Gamma_i^{\sigma} d \ln a_i \quad (14)$$

Because of the selection of the Gibbs dividing interface, the sum in eq 14 includes only solute species, and i denotes both neutral and charged species.

3.2. Modified Langmuir Adsorption Model. The most convenient way of determining the interfacial excess, Γ_i^{σ} , is by introducing an adsorption isotherm. Following our previous work on surface tension³⁷ and the methodology of Desnoyer et al.²⁵ and Li and Lu^{26,38} for modeling the vapor–liquid and liquid–liquid interfacial tensions of aqueous electrolyte solutions, an extended version of the Langmuir isotherm is used in this study. Further, it is coupled with a speciation-based thermodynamic model²⁸ within the framework of the Gibbs equation so that any change of interfacial tension due to chemical speciation can be explicitly represented as a function of electrolyte composition. The activities that are required for the calculation of interfacial tension are also determined from the thermodynamic model. The use of an extensively validated thermodynamic equilibrium model makes it possible for the interfacial tension model to be applicable over a wide range of electrolyte concentrations (i.e., from infinite dilution to the fused salt limit) and for any composition of solvent mixtures. For modeling interfacial tension, the adsorption isotherm needs to be applied to all solute species, namely, ions, ion pairs, and neutral molecules, that contribute to adsorption. Furthermore, the derivation of the expression for interfacial tension needs to take into account the interactions between solute species at the liquid–liquid interface.

In the classical Langmuir model, the equilibrium condition for the competitive adsorption of multiple species can be expressed by

$$k_{i,a}(1 - \sum_j \theta_j) a_i = k_{i,d} \theta_i \quad (15)$$

where $k_{i,a}$ and $k_{i,d}$ are the adsorption and desorption rate constants, respectively, of species i ; θ_i is the interfacial coverage fraction of the adsorbed species i ; and a_i is the activity of species i . Equation 15 can be rearranged to give

$$\theta_i = \frac{K_i a_i}{1 + \sum_j K_j a_j} \quad (16)$$

where $K_i = k_{i,a}/k_{i,d}$ is the adsorption equilibrium constant for species i . Assuming that the adsorption layer has a fixed capacity for a given species, the interfacial fraction θ_i can be related to the interfacial excess Γ_i^σ by introducing a maximum interfacial excess, $\Gamma_i^{\sigma,0}$,^{25,26,38} that is

$$\theta_i = \frac{\Gamma_i^\sigma}{\Gamma_i^{\sigma,0}} \quad (17)$$

Combining eqs 16 and 17 leads to the following expression for Γ_i^σ

$$\Gamma_i^\sigma = \Gamma_i^{\sigma,0} \frac{K_i a_i}{1 + \sum_j K_j a_j} \quad (18)$$

By substituting eq 18 into eq 14 and integrating the resulting expression from $a_i = 0$ (for which the liquid–liquid interfacial tension is that of the solute-free system, i.e., σ_{ms}) to the actual value of a_i , an expression for the effect of electrolyte concentration on interfacial tension is obtained as

$$\sigma - \sigma_{ms} = RT \sum_i \Gamma_i^{\sigma,0} \ln \left(1 - \frac{K_i a_i}{1 + \sum_j K_j a_j} \right) \quad (19)$$

Equation 19 was previously obtained by Li and Lu²⁶ and successfully applied to calculate the interfacial tension between organic solvents and aqueous electrolyte solutions at mostly moderate concentrations (up to ca. 5 *m*) by assuming a complete dissociation of the electrolytes. A further extension of eq 19 is necessary, however, when ionic concentrations in two-liquid-phase systems reach higher levels in either of the two liquid phases (e.g., in some ionic liquid + water mixtures or in aqueous two-phase systems) or when the effect of chemical speciation on interfacial tension becomes significant. To develop an extension of eq 19, it can be noted that interactions between adsorbed species in the interfacial region cannot be neglected, in particular at elevated concentrations of the solutes. Thus, in a multicomponent system, the interfacial excess of species i is likely to be affected by the presence of other species. Although classical approaches such as the Frumkin and related isotherms can account for the effects of interactions between species in an adsorbed layer,³⁹ such isotherms do not lead to an analytical expression for the interfacial tension when combined with the Gibbs equation (eq 14). Numerical integration of eq 14 in conjunction with a more complex isotherm is possible, but such an approach would require calculating the activities numerous times and would be very cumbersome, especially for process simulation applications. Therefore, following our previous work on vapor–liquid surface tension,³⁷ an extended expression for the electrolyte effect on interfacial tension is introduced to allow for pairwise interactions. The methodology used in the derivation of this extension was described in detail in a previous study.³⁷ In this extended expression, binary pairwise contributions are introduced, and the mean activities of species i and k , a_{ik} , are used rather than those for single species. This expression is an

empirical extension of eq 19 in which the single-species contributions $K_i a_i$ are replaced by pairwise contributions $K_{ik} a_{ik}$

$$\sigma - \sigma_{ms} = RT \sum_i \sum_k \Gamma_{ik}^{\sigma,0} \ln \left(1 - \frac{K_{ik} a_{ik}}{1 + \sum_j K_{jk} a_{jk}} \right) \quad (20)$$

where

$$a_{ik} = (a_i^{\nu_i} a_k^{\nu_k})^{1/\nu_{ik}} \quad (21)$$

$\nu_i = |z_i|$, $\nu_k = |z_k|$, and $\nu_{ik} = \nu_i + \nu_k$. For neutral species k (or i), $\nu_i = 1$ (or $\nu_k = 1$).

Because of the selection of the Gibbs dividing interface in the present study, eq 20 does not explicitly reflect the effects of the chemical nature of the solvent and its composition on the electrolyte-related increment in the interfacial tension, $\sigma - \sigma_{ms}$. However, the parameters in eq 20 (i.e., $\Gamma_{ik}^{\sigma,0}$ and K_{ik}) are unavoidably dependent on the solvent environment in which the electrolyte components find themselves. If such dependence were ignored, the interfacial tension increment due to the presence of electrolytes would be the same in all solvents at the same electrolyte activities. Therefore, eq 20 needs to be further extended to introduce the specificity of $\Gamma_{ik}^{\sigma,0}$ and K_{ik} to the solvent environment. In a previous study of the surface tension of mixed-solvent electrolyte systems,³⁷ the dependence of $\sigma - \sigma_{ms}$ on solvent composition was introduced by using a factor of $(x'_m x'_n)^{1/2}$, where x'_m and x'_n are the salt-free mole fractions of the solvents m and n , respectively. For liquid–liquid systems, the solvent composition at the interface is expected to be intermediate between those in the two liquid phases. Thus, the factor $(x'_m x'_n)^{1/2}$ needs to be redefined using the average mole fractions of the solvent components in the two liquid phases to approximate the composition in the interfacial region. Thus, the dependence of $\sigma - \sigma_{ms}$ on the solvent composition in a liquid–liquid system containing N_s solvent components and N_e solutes (ions, ion pairs, neutral molecules) is expressed as

$$\sigma - \sigma_{ms} = RT \sum_m^{N_s} \sum_n^{N_s} (\bar{x}_m \bar{x}_n)^{1/2} \sum_i^{N_e} \sum_k^{N_e} \Gamma_{ik, mn}^{\sigma,0} \ln \left(1 - \frac{K_{ik, mn} a_{ik}}{1 + \sum_j K_{jk, mn} a_{jk}} \right) \quad (22)$$

where

$$\bar{x}_m = \frac{1}{2}(x'_m{}^\alpha + x'_m{}^\beta), \quad \bar{x}_n = \frac{1}{2}(x'_n{}^\alpha + x'_n{}^\beta) \quad (22a)$$

and $x'_m{}^\alpha$, $x'_m{}^\beta$, $x'_n{}^\alpha$, and $x'_n{}^\beta$ are the salt-free mole fractions of solvents m and n in phases α and β , respectively. It should be noted here that the parameters $\Gamma_{ik}^{\sigma,0}$ and K_{ik} in eq 20 are redefined in eq 22 as $\Gamma_{ik, mn}^{\sigma,0}$ and $K_{ik, mn}$, respectively, to reflect the specificity of these parameters to the solvent environment.

4. PARAMETER EVALUATION

4.1. Parameters in the σ_{ms} Model for Nonelectrolyte Systems. The model for calculating the interfacial tension (σ_{ms}) of partially miscible nonelectrolyte mixtures (eqs 4–6) has an adjustable parameter, k_{ij} , that can be determined using experimental data for binary mixtures. The model does not impose any inherent constraints on the parameters k_{ij} and k_{ji} . However, for alkane + water systems and most polar + nonpolar pairs (e.g., water + arene, alcohol + toluene, and acetone + *n*-hexane) that were tested in this study, one of the k_{ij}

Table 1. Parameters of Eqs 4–6 and 23 for Selected Binary Liquid–Liquid Nonelectrolyte Mixtures

components		parameters		t (°C)	no. points	$\overline{\Delta\sigma}$ (mN·m ⁻¹)	ref(s)
i	j	$k_{ij}^{(0)}$	$k_{ij}^{(1)}$				
<i>n</i> -pentane ^a	water	0.782011	-3.17913×10^{-3}	15–149	14	1.158	75–79
<i>i</i> -pentane ^a	water	0.787278	-3.34465×10^{-3}	15–30	4	0.024	75
<i>n</i> -hexane ^a	water	0.685479	-5.72128×10^{-3}	10–60	29	0.554	6, 43, 75, 77–84
<i>n</i> -heptane ^a	water	0.548139	-2.88041×10^{-3}	10–50	19	0.337	6, 77–80, 82, 83
<i>n</i> -octane ^a	water	0.499618	-3.13330×10^{-3}	10–60	26	0.296	43, 77–80, 82, 83
<i>n</i> -nonane ^a	water	0.452275	-2.38740×10^{-3}	10–60	17	0.236	79, 80, 82, 83
<i>n</i> -decane ^a	water	0.417498	-1.78937×10^{-3}	10–176	44	0.972	43, 78–83, 85–89
<i>n</i> -C ₁₁ H ₂₄ ^a	water	0.376729	-2.20430×10^{-3}	15–55	14	0.205	79, 80, 82
<i>n</i> -C ₁₂ H ₂₆ ^a	water	0.361881	-3.18661×10^{-3}	10–60	20	0.345	43, 78–80, 82, 83
<i>n</i> -C ₁₃ H ₂₈ ^a	water	0.320000	0	20, 22	3	1.464	79, 82
<i>n</i> -C ₁₄ H ₃₀ ^a	water	0.308065	-2.63945×10^{-3}	20–50	5	1.227	43, 79, 82, 90
<i>n</i> -C ₁₅ H ₃₂ ^a	water	0.264839	0	20–25	6	1.544	43, 78, 79, 82, 83
<i>n</i> -C ₁₆ H ₃₄ ^a	water	0.235272	-2.39391×10^{-3}	20–80	9	0.793	43, 78, 79, 82, 83
<i>n</i> -C ₂₂ H ₄₆ ^a	water	0.138619	0	44.6	1	0.000	83
cyclohexane ^b	water	0.744518	-1.24771×10^{-3}	7–70	20	0.770	6, 87, 91, 92
benzene ^b	water	0.990853	0	7–176	37	0.488	6, 45, 68, 75, 77, 82, 85, 86, 88, 92–95
toluene ^b	water	0.797632	1.13649×10^{-3}	10–80	17	0.819	6, 77, 81, 95–97
ethylbenzene ^b	water	0.738741	0	20–80	6	1.024	6, 77, 97
<i>o</i> -xylene ^b	water	0.773514	0	20, 23	2	0.101	13, 47
decalin ^b	water	0.484498	0	25	1	0.000	44
phenol ^b	water	5.81920	2.25971×10^{-2}	5–66	15	0.023	56
<i>n</i> -butanol ^b	water	3.94941	8.50784×10^{-3}	–10–80	21	0.089	6, 66–69
heptanoic acid ^b	water	–0.277073	-9.51782×10^{-3}	5–65	14	0.073	98
<i>n</i> -butyl acetate ^b	water	0.830000	0	25, 50	2	0.383	2, 99
triethylamine ^b	water	14.0244	-3.12001×10^{-2}	20–60	10	0.286	56
CCl ₄ ^b	water	0.798132	0	20–25	6	0.631	6, 68, 88
CHCl ₃ ^b	water	0.977163	0	10–40	7	0.374	6, 68, 95
nitrobenzene ^b	hexane	7.83484	3.36921×10^{-2}	–2–20	27	0.027	56
benzene ^b	formic acid	2.42212	-4.07105×10^{-3}	10–60	6	0.718	56
octane ^b	phenol	8.13704	-2.16211×10^{-2}	27–53	11	0.037	56

^a $k_{ij}^{(0)} = 0$, $k_{ij}^{(1)} = 0$. ^b $k_{ij}^{(0)} = k_{ji}^{(0)}$, $k_{ij}^{(1)} = k_{ji}^{(1)}$.

or k_{ji} parameters was set equal to zero, for example, $k_{ij} \neq 0$ and $k_{ji} = 0$, whereas for most other systems, the equality of these parameters was assumed, namely, $k_{ij} = k_{ji}$. Only four polar/nonpolar pairs required two distinct parameters, that is, $k_{ij} \neq k_{ji}$. According to eqs 5 and 6, the interfacial tension has an inherent temperature dependence due to the temperature dependence of the liquid molar volumes of the mixture components, ν_i^0 . However, the temperature dependence of the liquid volumes might not provide a sufficient variation of σ_{ms} with temperature because the change in interfacial tension with temperature can be more or less pronounced than that implied by the liquid molar volumes. Thus, an additional temperature dependence of the binary parameter k_{ij} is introduced, when necessary, to represent the variation of σ_{ms} with temperature

$$k_{ij} = k_{ij}^{(0)} \exp[k_{ij}^{(1)}(T - T_0)] \quad (23)$$

where T is in Kelvin and $T_0 = 273.15$ K.

4.2. Parameters $\Gamma_{ik}^{\sigma,0}$ and K_{ik} . Most interfacial tension data that are available in the literature for liquid–liquid systems containing electrolytes are limited to a single temperature (i.e., 25 °C) or cover only a narrow temperature range. Therefore, an explicit temperature dependence of the binary parameters $\Gamma_{ik}^{\sigma,0}$ and K_{ik} is necessary only for systems for which the data cover relatively wide temperature ranges (e.g., 20–50 °C in the case of ionic liquid + water systems). The dependence of $\Gamma_{ik}^{\sigma,0}$

and K_{ik} on temperature can be expressed by the simple functions

$$\Gamma_{ik}^{\sigma,0} = \Gamma_{ik}^{\sigma,01} + \frac{\Gamma_{ik}^{\sigma,02}}{T} \quad (24a)$$

$$K_{ik} = K_{ik}^{(1)} + \frac{K_{ik}^{(2)}}{T} \quad (24b)$$

It should be noted that the parameters $\Gamma_{ik}^{\sigma,0}$ and K_{ik} are solvent-dependent, as implied by eqs 22 and 22a. For example, these parameters can be different for a given species pair in water + benzene and in water + hexane mixtures.

5. RESULTS AND DISCUSSION

5.1. Liquid–Liquid Interfacial Tension (σ) in Non-electrolyte Systems and Variation of σ with Mutual Solubility. Experimental data for a number of binary and ternary liquid–liquid systems were used to validate the mixing rule described in section 2. For all systems for which the interfacial tension model was tested, thermodynamic model parameters²⁸ were first developed to provide appropriate liquid–liquid equilibrium compositions as input for interfacial tension modeling. Table 1 lists the parameters k_{ij} for selected binary systems, together with the average error, defined by

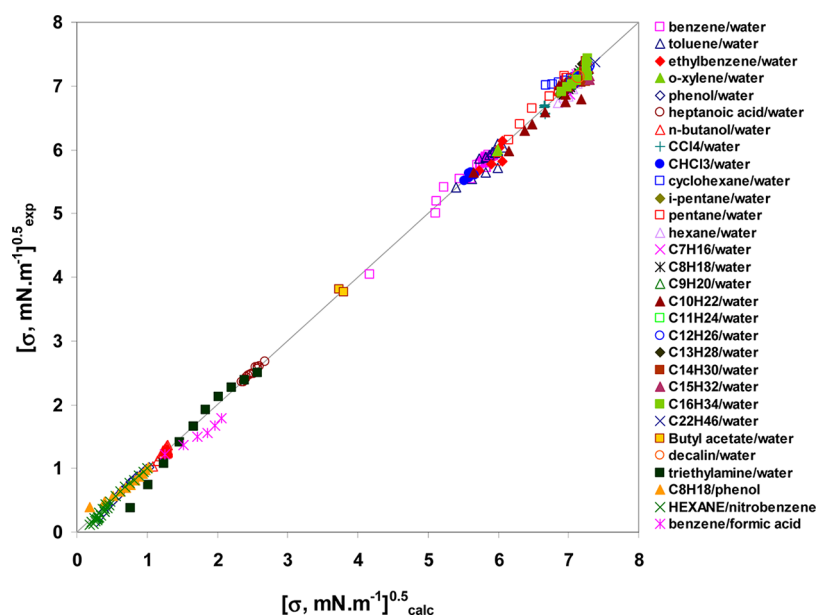


Figure 1. Comparison of the calculated interfacial tension with literature values for binary liquid–liquid systems. References to the literature data are given in Table 1.

$$\overline{\Delta\sigma} = \left(\sum_k^n |\sigma_{\text{exp},k} - \sigma_{\text{calc},k}| \right) / n \quad (25)$$

where n is the number of experimental data points. Literature data sources are also included in the table. These results are further visualized in Figure 1, which compares the calculated interfacial tensions with experimental data.

Using the parameters determined from binary data, the interfacial tensions of ternary systems can be predicted. For most of the ternary systems for which interfacial tension data are reported, only a few systems have more than one constituent binary subsystem for which interfacial tension data are available. Table 2 summarizes the predicted results for

Table 2. Results for Ternary Mixtures Predicted Using the Binary Parameters in Table 1

solvent mixture			t (°C)	no. points	$\overline{\Delta\sigma}$ (mN·m ^{−1})	ref
i	j	k				
benzene	water	formic acid	25	8	0.224	45
CCl ₄	water	<i>n</i> -heptane	25	7	3.801	50
<i>n</i> -hexane	water	<i>n</i> -C ₁₀ H ₂₂	25, 50	6	0.161	43

three such ternary systems using the binary parameters listed in Table 1. The predicted and experimental interfacial tensions are in good agreement, as illustrated in Figure 2.

When experimental data and, hence, binary parameters for some of the constituent binary systems are not available, the interfacial tension data for ternary systems were used to determine the missing parameters for the pairs for which binary data are unavailable or cannot be directly determined (e.g., in the ternary system benzene + water + ethanol, the water + ethanol binary is fully miscible, and therefore, no liquid–liquid interfacial tension exists). In general, for a ternary system, only the parameters for one missing pair are necessary to model the interfacial tension. The pair that is most prone to form two liquid phases (e.g., a polar/nonpolar pair) is then selected to determine the parameters k_{ik} by fitting the σ data in ternary

systems. Table 3 summarizes the interfacial tension results for such systems. Thus, the parameters for the pair $\{i, k\}$ were determined using data for ternary systems, whereas those for $\{i, j\}$ were taken from Table 1. The interfacial tension results that were obtained using the parameters in Tables 1 and 3 are further compared with literature data in Figure 3 for five ternary liquid–liquid systems of the type benzene + water + polar organic (where polar organic = acetone, acetic acid, *i*-propanol, ethanol, and methanol). Strong effects of the polar organic components on the interfacial tension are evident, as these components cause a significant decrease in the interfacial tension upon being added to the benzene + water mixtures.

The results that were obtained for the nonelectrolyte liquid–liquid systems indicate that the model (eqs 4–6) can accurately reproduce the experimental data and is capable of predicting interfacial tension in ternary mixtures using parameters obtained from data for binary subsystems (cf. Figure 2). It is noteworthy that the values of the parameter k_{ij} are usually positive, with the exception of that for the heptanoic acid + water mixture. The positive values of these parameters indicate a certain augmentation of the interfacial molar volumes of the components and, consequently, their interfacial molar areas compared to those for the pure liquids. This can be attributed to systematic variations of the intermolecular interactions on the interface, which result from the dissimilarity of the two fluids in the system. These parameters have a general trend of becoming less positive as the number of carbons (or the molecular weight) increases. This trend can be observed for alkanes and for alkylbenzenes, as seen in Table 1 for their mixtures with water. An increase in the number of carbons causes an increase in the interfacial tension, which is accompanied by a simultaneous decrease in the solubility of the hydrocarbon in water. This is demonstrated in Figure 4, where both interfacial tension and hydrocarbon solubility in water are plotted as functions of the number of carbons. The increase in the interfacial tension and, hence, in the interfacial Gibbs free energy appears to be a result of an augmentation in intermolecular interactions at the interface due to an increased dissimilarity in the coexisting fluids as the hydrocarbon chain

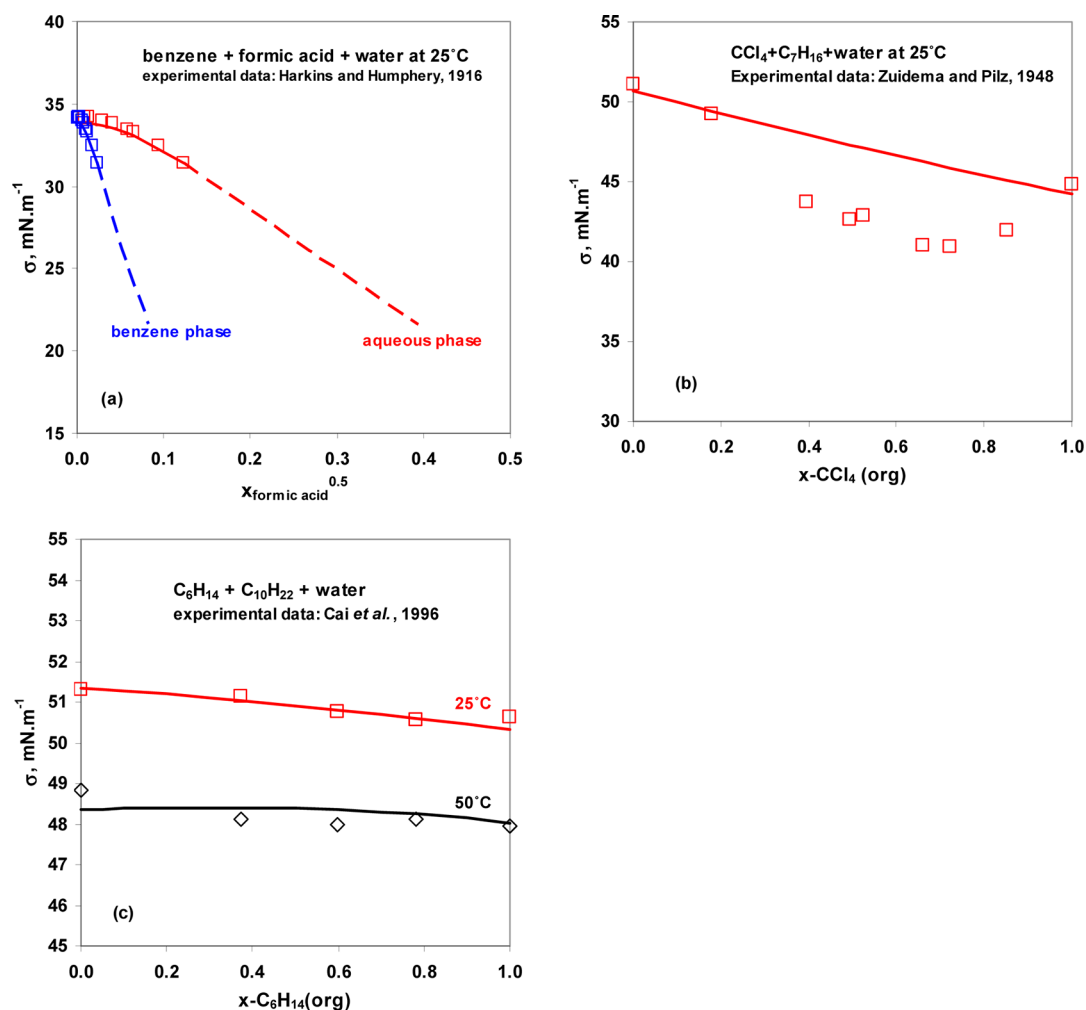


Figure 2. Predicted interfacial tensions in ternary liquid–liquid systems: (a) benzene + formic acid + water, (b) $n\text{-C}_7\text{H}_{16}$ + CCl_4 + water, (c) $n\text{-C}_6\text{H}_{14}$ + $n\text{-C}_{10}\text{H}_{22}$ + water. The symbols are from the literature,^{43,45,50} and the lines were predicted using eqs 4–6 and the parameters in Table 1.

length increases. At the same time, as the number of carbons increases, the liquid molar volume contribution (v_l^0) to the interfacial molar volume (v_i^{int}), as defined by eq 6, also increases. The increases in the interfacial molar volume (v_i^{int}) with number of carbons can be largely explained by the increase in the liquid molar volume, leading to a decreased, although still positive, binary parameter k_{ij} as the v_j^0 and k_{ij} parameters partially compensate each other.

The strong relationship between the mutual solubility and the interfacial tension can also be demonstrated by analyzing the three binary systems phenol + water, triethylamine + water, and n -butanol + water. The results for these systems are shown in Figures 5–7. These results show that the interfacial tension decreases in lockstep with increasing mutual solubility as the temperature changes. In the phenol + water mixtures (Figure 5), the mutual solubility of phenol and water increases, whereas σ decreases with temperature. The interfacial tension drops to zero as the temperature approaches the upper critical solution temperature (UCST), above which the components become fully miscible. Conversely, the triethylamine + water system exhibits a lower critical solution temperature (LCST), as shown in Figure 6. In this case, the interfacial tension is zero at the LCST point at which complete miscibility is reached and increases with temperature as the miscibility gap widens (or, equivalently, the mutual solubility decreases). For the n -butanol

+ water system (Figure 7), the solubility of n -butanol in water shows a minimum. Correspondingly, σ exhibits a maximum as a function of temperature and then decreases as the miscibility gap shrinks with a further increase in temperature. The interfacial tension model accurately reproduces the variation of σ with temperature on the basis of the thermodynamic mixed-solvent electrolyte (MSE) model, which provides the liquid–liquid equilibrium compositions. Thus, both σ and LLE can be reproduced simultaneously.

5.2. Effects of the Ionic Concentration on the Interfacial Tension. Applications of the new interfacial tension model to systems with ionic components focused on two classes of mixtures: (1) electrolytes in “base systems” in which interfacial tension is well-defined and experimentally known (e.g., in nonelectrolyte liquid–liquid systems) and (2) ionic systems for which a base system of an immiscible nonelectrolyte mixture does not exist or cannot be determined. Systems that belong to the first class include organic + water + salt mixtures where the organic + water subsystem is a partially miscible base system. Examples of the second class include ionic liquid + water mixtures and aqueous two-phase systems such as poly(ethylene glycol) + water + salt ternaries. As a first step toward understanding and predicting the liquid–liquid interfacial tension as a function of ionic additives, only systems with simple electrolytes were studied in the present work. Ionic

Table 3. Results for Ternary Mixtures Predicted Using the Binary Parameters in Table 1^a

solvent mixture			parameters ^b		<i>t</i> (°C)	no. points	$\overline{\Delta\sigma}$ (mN·m ⁻¹)	ref(s)
<i>i</i>	<i>j</i>	<i>k</i>	$k_{ik}^{(0)}$	$k_{ki}^{(0)}$				
benzene	water	acetic acid	47.3520	1.85611	25	10	0.174	6, 45
benzene	water	butyric acid	11.1387	11.1387	25	6	1.133	45
benzene	water	acetone	34.6726	0	30	6	0.849	51
benzene	water	methanol	41.5975	0	25	14	0.627	51, 53
benzene	water	ethanol	82.3613	0	20, 25	14	1.092	52, 54
benzene	water	<i>i</i> -propanol	104.695	0	25	18	0.837	52, 53
benzene	water	<i>n</i> -propanol	134.518	4.75045	30	8	0.445	2
benzene	water	NH ₃	1.29302	1.29302	25	3	0.076	45
<i>n</i> -hexane	water	acetone	164.342	0	25	11	1.174	53
<i>n</i> -hexane	water	ethanol	137.350	0	20	8	0.324	54
<i>n</i> -hexane	water	<i>i</i> -propanol	282.062	1.70347	25	11	0.702	53
<i>n</i> -hexane	water	<i>n</i> -propanol	419.674	2.82100	25	5	0.850	6
<i>n</i> -heptane	water	<i>n</i> -propanol	585.015	0	25	5	1.255	6
toluene	water	ethanol	95.5544	0	25	7	0.823	52
toluene	water	<i>i</i> -propanol	122.201	0	25	6	0.694	52
toluene	water	<i>n</i> -propanol	165.892	0	25	7	0.639	52
CCl ₄	water	<i>n</i> -propanol	174.652	0	20	6	0.634	51
CHCl ₃	water	acetone	9.58169	0	25	5	1.496	6
cyclohexane	water	<i>i</i> -propanol	212.194	0	21, 25	12	0.720	52, 100
<i>n</i> -butyl acetate	water	<i>n</i> -propanol	77.6398	0	50	4	1.399	99

^aInterfacial tension data for ternary systems were used to determine additional binary parameters for the pairs $\{i, k\}$ for which no data on the corresponding binary systems were available. ^b $k_{ik}^{(1)} = k_{ki}^{(1)} = 0$ for all $\{i, k\}$ pairs.

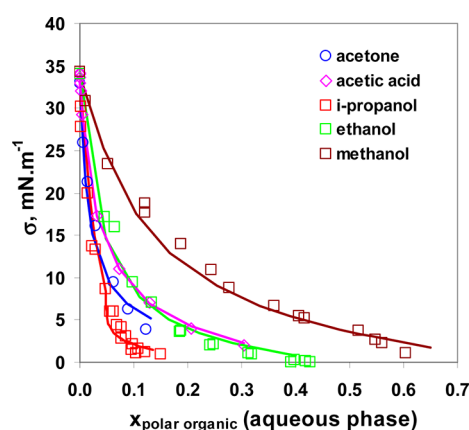


Figure 3. Variations of the interfacial tension with the equilibrium mole fraction of the polar organic component in the aqueous phase of the ternary liquid–liquid systems polar organic + benzene + water (25 °C), where polar organic = acetone, acetic acid, *i*-propanol, ethanol, and methanol. The symbols denote literature data,^{6,45,51–54} and the lines were calculated using eqs 4–6.

surfactants were not considered here because they have specific structural and compositional characteristics and physicochemical properties that require a different treatment.

Experimental interfacial tension data for systems containing ionizable components are available from various literature sources^{40–49} but are much less extensive than surface tension data for vapor–liquid systems. The majority of the available data have been reported for systems that contain a single electrolyte component. Published data for systems with mixed electrolytes are sparse.^{25,43} Moreover, it should be noted that thermodynamic model parameters²⁸ must be developed prior to modeling interfacial tension to provide the necessary speciation, activity coefficients, and miscibility gap compositions. However, in some cases, the exact chemical composition

of the organic solvent is not explicitly stated,²⁵ and relevant liquid–liquid equilibrium data and thermochemical properties that are necessary to construct a phase equilibrium model as a thermodynamic foundation for modeling interfacial tension are lacking. Thus, in the present study, the interfacial tension model is applied only to systems for which the relevant thermodynamic properties can be calculated.²⁸ Nonetheless, the available literature data for systems with well-defined solvents and electrolyte solutes provide a sound basis for testing the new model.

Table 4 lists the adjustable parameters in eqs 22, 24a, and 24b, namely, $\Gamma_{ik}^{\sigma,0}$ and K_{ik} , for selected systems containing ionic components. If necessary, the parameters of eqs 4–6 are also included (e.g., for ionic liquid + water systems).

The performance of the model for aqueous salt + organic solvent systems is illustrated in Figures 8 and 9. In Figure 8, the calculated interfacial tension is compared with literature data for the systems *n*-hexane + water + electrolyte, *n*-dodecane + water + electrolyte, and benzene + water + electrolyte as a function of electrolyte concentration for various salts and acids and a base. Figure 9 shows the results for various combinations of organic solvents and aqueous NaCl. These results show that the effects of electrolytes on interfacial tension can differ depending on the system. For the aqueous electrolyte + organic systems studied in this work, interfacial tension increases with electrolyte concentration with the exception of the aqueous sodium chloride + *o*-xylene system, for which a decrease with salt concentration is observed (Figure 9). The aqueous sulfuric acid + benzene system (Figure 8d) shows a decrease in interfacial tension with acid concentration at low H₂SO₄ molalities. Then, the interfacial tension reaches a shallow minimum and rises with a further increase in the acid concentration. Such behavior can be associated with changes in the speciation of sulfuric acid solutions. For this system, it is necessary to introduce the $\Gamma_{ik}^{\sigma,0}$ and K_{ik} parameters for both the

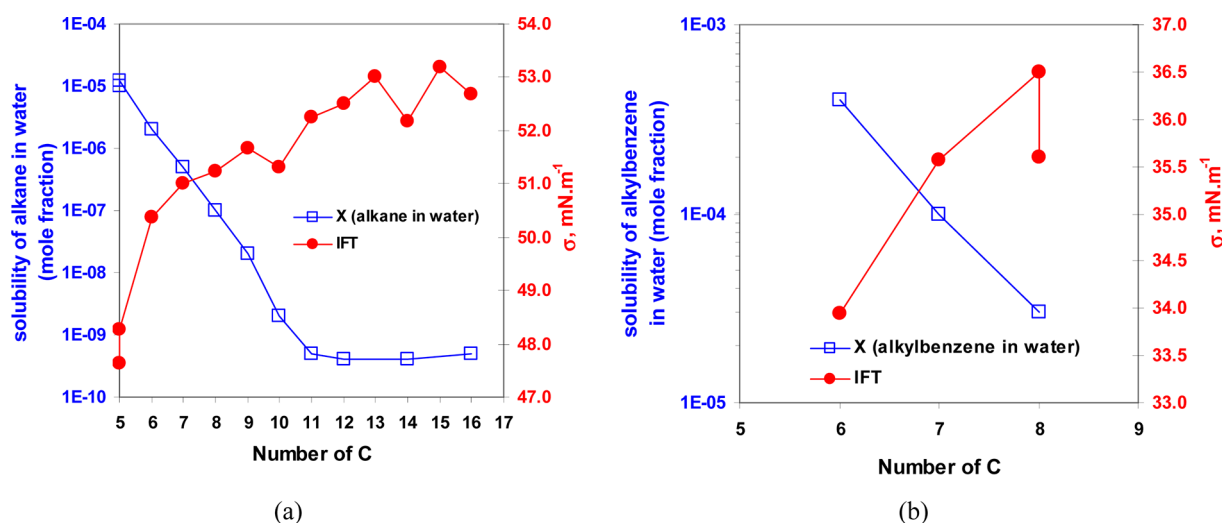


Figure 4. Variations of the interfacial tension and solubility of hydrocarbons in water at 25 °C with the number of carbons in the hydrocarbon molecules in mixtures of (a) alkanes + water (including *n*-alkanes, *i*-pentane, and cyclohexane) and (b) alkylbenzenes + water (including benzene, toluene, ethylbenzene, and *o*-xylene). The values of interfacial tension were calculated using eqs 11a–11c, 12, and 13a–13c based on literature data, and the solubilities are the averaged experimental data from the compilation of Frenkel et al.⁵⁵

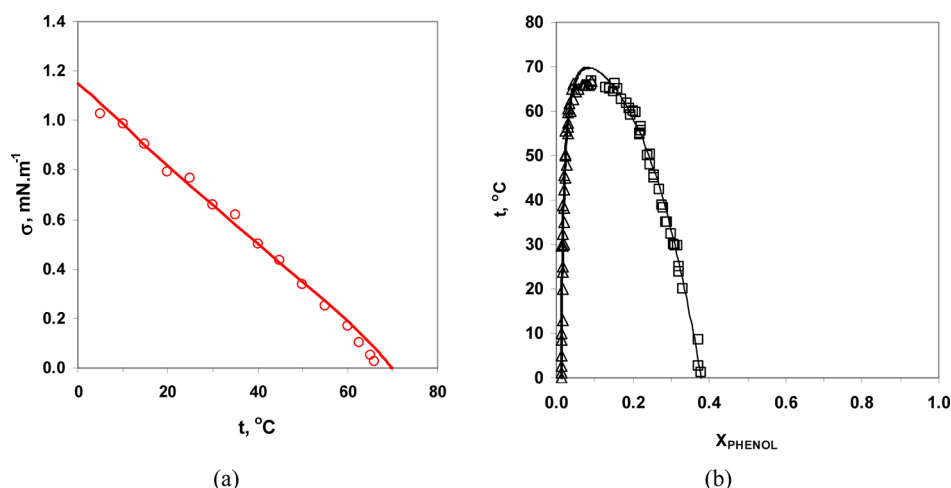


Figure 5. Variations with temperature of (a) the interfacial tension and (b) the corresponding mutual solubility in phenol + water mixtures. In panel a, the symbols denote experimental data,⁵⁶ and the line was calculated using eqs 4–6. In panel b, the symbols denote experimental mutual solubilities,^{57–62} and the lines were calculated using the MSE model.^{28,33}

$\text{H}_3\text{O}^+/\text{HSO}_4^-$ and $\text{H}_3\text{O}^+/\text{SO}_4^{2-}$ pairs to represent the variation of interfacial tension with acid concentration.

In our previous work on modeling surface tension,³⁷ negative values of $\Gamma_{ik}^{\sigma,0}$ were observed for systems in which surface tension increases with electrolyte concentration, thus indicating a negative adsorption (or deficiency) of the electrolyte on the solution surface. Conversely, a positive $\Gamma_{ik}^{\sigma,0}$ value led to a decrease in surface tension with electrolyte concentration. However, such trends were not observed for all systems in modeling interfacial tension. This is due to the fact that the value of σ_{ms} , namely, the baseline interfacial tension in the absence of electrolytes, is calculated based on the equilibrium concentrations of nonelectrolyte components on a salt-free basis. Such salt-free nonelectrolyte compositions in electrolyte-containing systems can be different from the equilibrium compositions in the absence of salts, because of the electrolyte effects on liquid–liquid equilibria that are associated with salting-in (increased solubility) or salting-out (reduced solubility) effects. For systems with a salting-out effect, the

reduced mutual solubility in the presence of an electrolyte leads to a greater value of σ_{ms} compared to that obtained for the equilibrium composition in the absence of the electrolyte. Thus, when the ionic binary parameters ($\Gamma_{ik}^{\sigma,0}$ and K_{ik}) are regressed to reproduce the variation of interfacial tension with electrolyte concentration, the elevated σ_{ms} value can result in either a positive or a negative $\Gamma_{ik}^{\sigma,0}$ value, depending on how strong the salting-out effect is. This is demonstrated in Figure 10, where the interfacial tensions in the systems benzene + aqueous HCl and benzene + aqueous NaCl are plotted as functions of the salt concentration. To elucidate the effect of salting in or salting out on the interfacial tension, predictions obtained with zero values of $\Gamma_{ik}^{\sigma,0}$ and K_{ik} (which are equivalent to σ_{ms} in eq 22) are shown as dashed lines. They are compared in Figure 10 with the results obtained using regressed $\Gamma_{ik}^{\sigma,0}$ and K_{ik} values in Table 4 (σ , solid lines). For the system benzene + aqueous HCl, the calculated σ_{ms} value, based on the equilibrium salt-free concentrations of the solvent components (benzene and water), is greater than σ (cf. Figure 10a), and therefore, a

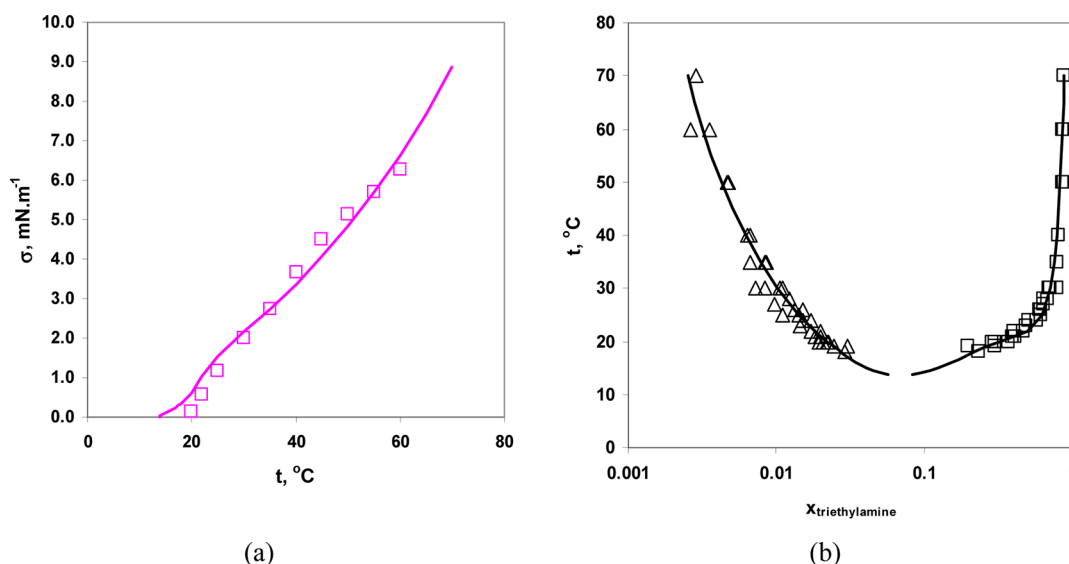


Figure 6. Variations with temperature of (a) the interfacial tension and (b) the corresponding mutual solubility in triethylamine + water mixtures. In panel a, the symbols denote experimental data⁵⁶ and the line was calculated using eqs 4–6. In panel b, the symbols denote experimental mutual solubilities,^{63–65} and the lines were calculated using the MSE model.^{28,33}

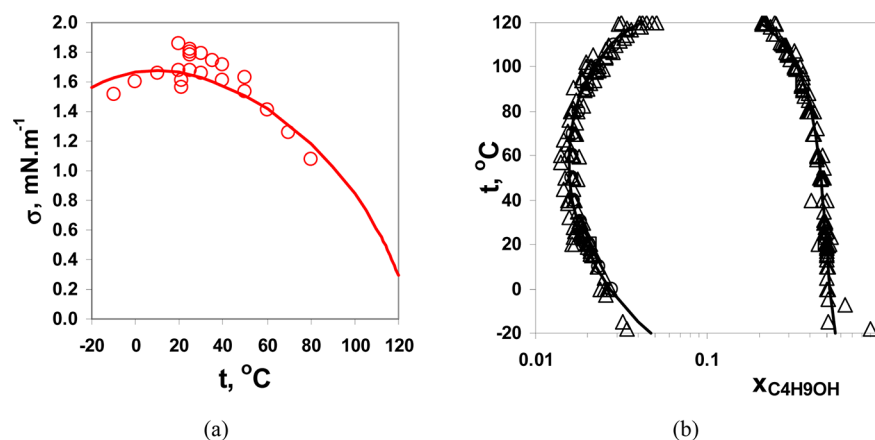


Figure 7. Variations with temperature of (a) the interfacial tension and (b) the corresponding mutual solubility in *n*-butanol + water mixtures. In panel a, the symbols denote experimental data,^{6,66–69} and the line was calculated using eqs 4–6. In panel b, the symbols denote experimental mutual solubilities,^{58,70–74} and the lines were calculated using the MSE model.^{28,33}

positive $\Gamma_{ik}^{\sigma,0}$ value is obtained for the $\{\text{H}_3\text{O}^+, \text{Cl}^-\}$ pair. In contrast, for the system benzene + aqueous NaCl, the σ_{ms} values that incorporate the salting-out effect are smaller than the total σ values (Figure 10b), and therefore, a negative $\Gamma_{ik}^{\sigma,0}$ is obtained for the $\{\text{Na}^+, \text{Cl}^-\}$ pair. Thus, $\Gamma_{ik}^{\sigma,0}$ in the present model represents the excess (positive increment) or deficiency (negative increment) of the electrolyte at the interface using, as a reference state, a salt-free liquid–liquid system whose composition varies with the electrolyte concentration. As shown in Figure 10, the σ values that are predicted without the $\Gamma_{ik}^{\sigma,0}$ and K_{ik} parameters (i.e., the dashed lines) capture the trend of interfacial tension with electrolyte concentration based solely on the salt effects on liquid–liquid equilibria. Thus, for systems for which no data are available, eqs 4–6 and 22 can predict a reasonable interfacial tension trend as long as accurate liquid–liquid equilibria can be obtained from thermodynamics.²⁸ The internal linkage with phase equilibria, as quantified by the salting-in or salting-out effects, provides the present model with a distinctive capability to predict the variation of σ with electrolyte concentration. This is an advantage of the new

model compared to other existing interfacial tension models for electrolyte systems.

For systems containing ionic liquids and water, both water and the undissociated ionic liquid molecules [e.g., BMIM·N(CF₃SO₂)₂⁰ and EMIM·N(CF₃SO₂)₂⁰] need to be treated as solvent components because of the strong ion association effects that are evident in the treatment of thermodynamic properties.³⁴ At the same time, the dissociated cation and anion are treated as solute species because they can exist in significant amounts in both liquid phases. In such systems, speciation can change dramatically with the concentration of the ionic liquid.³⁴ The binary parameters that are used in the model for this type of systems include the $\Gamma_{ik}^{\sigma,0}$ and K_{ik} parameters between the cation and the anion in eq 22 and the k_{ij} parameter between the solvent components [e.g., H₂O and BMIM·N(CF₃SO₂)₂⁰] in eqs 4–6. For example, the best fit for the system BMIM·N(CF₃SO₂)₂ + H₂O was obtained when the parameters $\Gamma_{\text{BMIM,NTf}_2/\text{H}_2\text{O,IL}_1}^{\sigma,0}$, $K_{\text{BMIM,NTf}_2/\text{H}_2\text{O,IL}_1}$, and $k_{\text{H}_2\text{O,IL}_1}$ were introduced [where $\text{NTf}_2 = \text{N}(\text{CF}_3\text{SO}_2)_2^-$, $\text{IL}_1 = \text{BMIM} \cdot \text{N}(\text{CF}_3\text{SO}_2)_2^0$, and $k_{\text{IL}_1,\text{H}_2\text{O}} = k_{\text{H}_2\text{O,IL}_1}$]. These parameters are listed in Table 4. As

Table 4. Interaction Parameters for Modeling the Interfacial Tension of Selected Systems Containing Electrolytes

system and conditions	parameters	no. points	$\frac{\Delta\sigma}{\Delta T}$ (mN·m ⁻¹)	ref(s)
NaOH + water + <i>n</i> -hexane $t = 25$ °C, $m_{\text{NaOH}}^{\text{max}} = 0.7$	$\Gamma_{\text{NaOH}/\text{H}_2\text{O}/\text{C}_6\text{H}_{14}}^0 = -2.59672$ $K_{\text{NaOH}/\text{H}_2\text{O}/\text{C}_6\text{H}_{14}}^{(1)} = 1.27098 \times 10^{-2}$	5	0.087	48
KNO ₃ + water + <i>n</i> -hexane $t = 25$ °C, $m_{\text{KNO}_3}^{\text{max}} = 0.7$	$\Gamma_{\text{KNO}_3/\text{H}_2\text{O}/\text{C}_6\text{H}_{14}}^0 = -0.372560$ $K_{\text{KNO}_3/\text{H}_2\text{O}/\text{C}_6\text{H}_{14}}^{(1)} = 4.69722 \times 10^{-2}$	7	0.067	48
LiCl + water + <i>n</i> -hexane $t = 25$ °C, $m_{\text{LiCl}}^{\text{max}} = 0.93$	$\Gamma_{\text{LiCl}/\text{H}_2\text{O}/\text{C}_6\text{H}_{14}}^0 = -0.507210$ $K_{\text{LiCl}/\text{H}_2\text{O}/\text{C}_6\text{H}_{14}}^{(1)} = 2.67178 \times 10^{-2}$	8	0.067	48
KCl + water + <i>n</i> -hexane $t = 25$ °C, $m_{\text{KCl}}^{\text{max}} = 0.5$	$\Gamma_{\text{KCl}/\text{H}_2\text{O}/\text{C}_6\text{H}_{14}}^0 = -0.372560$ $K_{\text{KCl}/\text{H}_2\text{O}/\text{C}_6\text{H}_{14}}^{(1)} = 4.69722 \times 10^{-2}$	6	0.058	48
NaCl + water + <i>n</i> -hexane $t = 25, 50$ °C; $m_{\text{NaCl}}^{\text{max}} = 0.88$	$\Gamma_{\text{NaCl}/\text{H}_2\text{O}/\text{C}_6\text{H}_{14}}^0 = -1.04090$ $K_{\text{NaCl}/\text{H}_2\text{O}/\text{C}_6\text{H}_{14}}^{(1)} = 5.11851 \times 10^{-2}$	9	0.205	43, 48
NaCl + CaCl ₂ + water + <i>n</i> -hexane $t = 25, 50$ °C; $m_{\text{NaCl}} = 0.44$, $m_{\text{CaCl}_2} = 0.70$	$\Gamma_{\text{CaCl}_2/\text{H}_2\text{O}/\text{C}_6\text{H}_{14}}^0 = 0$ $K_{\text{CaCl}_2/\text{H}_2\text{O}/\text{C}_6\text{H}_{14}}^{(1)} = 0$	2	0.154	43
NaCl + water + <i>n</i> -C ₁₀ H ₂₂ $t = 25, 50$ °C; $m_{\text{NaCl}} = 0.88$	$\Gamma_{\text{NaCl}/\text{H}_2\text{O}/\text{C}_{10}\text{H}_{22}}^0 = -1.55780$ $K_{\text{NaCl}/\text{H}_2\text{O}/\text{C}_{10}\text{H}_{22}}^{(1)} = 4.69821 \times 10^{-2}$	2	0.186	43
NaCl + CaCl ₂ + water + <i>n</i> -C ₁₀ H ₂₂ $t = 25, 50$ °C; $m_{\text{NaCl}} = 0.44$, $m_{\text{CaCl}_2} = 0.70$	$\Gamma_{\text{CaCl}_2/\text{H}_2\text{O}/\text{C}_{10}\text{H}_{22}}^0 = 0$ $K_{\text{CaCl}_2/\text{H}_2\text{O}/\text{C}_{10}\text{H}_{22}}^{(1)} = 0$	2	0.098	43
NaCl + water + <i>o</i> -xylene $t = 23$ °C, $m_{\text{NaCl}}^{\text{max}} = 0.5$	$\Gamma_{\text{NaCl}/\text{H}_2\text{O}/\text{o-xylene}}^0 = 4.60789$ $K_{\text{NaCl}/\text{H}_2\text{O}/\text{o-xylene}}^{(1)} = 5.52935 \times 10^{-2}$	4	0.596	47
NaCl + water + <i>n</i> -octane $t = 20, 25, 50$ °C; $m_{\text{NaCl}}^{\text{max}} = 5$	$\Gamma_{\text{NaCl}/\text{H}_2\text{O}/\text{C}_8\text{H}_{18}}^0 = -0.601829$ $K_{\text{NaCl}/\text{H}_2\text{O}/\text{C}_8\text{H}_{18}}^{(1)} = 4.07141 \times 10^{-2}$	7	0.985	43, 46
H ₂ SO ₄ + water + benzene $t = 25$ °C, $m_{\text{H}_2\text{SO}_4}^{\text{max}} = 0.6$	$\Gamma_{\text{H}_2\text{SO}_4/\text{H}_2\text{O}/\text{C}_6\text{H}_6}^0 = -3.05278$ $K_{\text{H}_2\text{SO}_4/\text{H}_2\text{O}/\text{C}_6\text{H}_6}^{(1)} = 2.48461 \times 10^{-3}$ $\Gamma_{\text{H}_2\text{SO}_4/\text{H}_2\text{O}/\text{C}_6\text{H}_6}^0 = 1.89056$ $K_{\text{H}_2\text{SO}_4/\text{H}_2\text{O}/\text{C}_6\text{H}_6}^{(1)} = 3.25120 \times 10^{-2}$	7	0.014	45
HCl + water + benzene $t = 25$ °C, $m_{\text{HCl}}^{\text{max}} = 0.99$	$\Gamma_{\text{H}_2\text{O}/\text{H}_2\text{O}/\text{C}_6\text{H}_6}^0 = 0.644413$ $K_{\text{H}_2\text{O}/\text{H}_2\text{O}/\text{C}_6\text{H}_6}^{(1)} = 1.00663 \times 10^{-2}$	5	0.024	45
NaCl + water + benzene $t = 25$ °C, $m_{\text{NaCl}}^{\text{max}} = 1.03$	$\Gamma_{\text{NaCl}/\text{H}_2\text{O}/\text{C}_6\text{H}_6}^0 = -1.24254$ $K_{\text{NaCl}/\text{H}_2\text{O}/\text{C}_6\text{H}_6}^{(1)} = 1.60413 \times 10^{-2}$	7	0.064	45
KCl + water + decalin $t = 25$ °C, $m_{\text{KCl}}^{\text{max}} = 1.0$	$\Gamma_{\text{KCl}/\text{H}_2\text{O}/\text{C}_{10}\text{H}_{18}}^0 = -0.204500$ $K_{\text{KCl}/\text{H}_2\text{O}/\text{C}_{10}\text{H}_{18}}^{(1)} = 0.154447$	12	0.020	44
BaCl ₂ + water + decalin $t = 25$ °C, $m_{\text{BaCl}_2}^{\text{max}} = 0.5$	$\Gamma_{\text{BaCl}_2/\text{H}_2\text{O}/\text{C}_{10}\text{H}_{18}}^0 = -3.03502$ $K_{\text{BaCl}_2/\text{H}_2\text{O}/\text{C}_{10}\text{H}_{18}}^{(1)} = 2.19253 \times 10^{-2}$	11	0.023	44
AlCl ₃ + water + decalin $t = 25$ °C, $m_{\text{AlCl}_3}^{\text{max}} = 0.17$	$\Gamma_{\text{AlCl}_3/\text{H}_2\text{O}/\text{C}_{10}\text{H}_{18}}^0 = -1.13635$ $K_{\text{AlCl}_3/\text{H}_2\text{O}/\text{C}_{10}\text{H}_{18}}^{(1)} = 0.145226 \times 10^{-01}$	11	0.164	44
Na ₂ SO ₄ + water + C ₁₂ H ₂₆ $t = 20$ °C, $m_{\text{KNO}_3}^{\text{max}} = 1.02$	$\Gamma_{\text{KNO}_3/\text{H}_2\text{O}/\text{C}_{12}\text{H}_{26}}^0 = -2.66409$ $K_{\text{KNO}_3/\text{H}_2\text{O}/\text{C}_{12}\text{H}_{26}}^{(1)} = 4.96073 \times 10^{-2}$	4	0.179	42
LiCl + water + C ₁₂ H ₂₆ $t = 20$ °C, $m_{\text{LiCl}}^{\text{max}} = 0.87$	$\Gamma_{\text{LiCl}/\text{H}_2\text{O}/\text{C}_{12}\text{H}_{26}}^0 = -0.614905$ $K_{\text{LiCl}/\text{H}_2\text{O}/\text{C}_{12}\text{H}_{26}}^{(1)} = 5.90431 \times 10^{-2}$	8	0.040	42
KCl + water + C ₁₂ H ₂₆ $t = 20$ °C, $m_{\text{KCl}}^{\text{max}} = 1.34$	$\Gamma_{\text{KCl}/\text{H}_2\text{O}/\text{C}_{12}\text{H}_{26}}^0 = -0.568870$ $K_{\text{KCl}/\text{H}_2\text{O}/\text{C}_{12}\text{H}_{26}}^{(1)} = 7.22644 \times 10^{-2}$	4	0.064	42

Table 4. continued

system and conditions	parameters	no. points	$\overline{\Delta\sigma}$ (mN·m ⁻¹)	ref(s)
NaCl + water + C ₁₂ H ₂₆ $t = 20, 25, 50$ °C; $m_{\text{NaCl}}^{\text{max}} = 1.02$	$\Gamma_{\text{NaCl/H}_2\text{O/C}_{12}\text{H}_{26}}^0 = -1.66598$ $K_{\text{NaCl/H}_2\text{O/C}_{12}\text{H}_{26}}^{(1)} = 2.26761 \times 10^{-2}$	14	0.086	42, 43
(NH ₄) ₂ SO ₄ + PEG4000 + water $t = 25$ °C, wt% ^{max} _{(NH₄)₂SO₄} = 12.5, wt% ^{max} _{PEG} = 12.9	$\Gamma_{\text{NH}_4\text{SO}_4/\text{H}_2\text{O/PEG}}^0 = -8.59217$ $K_{\text{NH}_4\text{SO}_4/\text{H}_2\text{O/PEG}}^{(1)} = 1.44652 \times 10^{-2}$	4	0.061	41
K ₂ HPO ₄ + PEG4000 + water $t = 25$ °C, wt% ^{max} _{K₂HPO₄} = 11.43, wt% ^{max} _{PEG} = 12.48	$\Gamma_{\text{K}_2\text{HPO}_4/\text{H}_2\text{O/PEG}}^0 = -5.80800$ $K_{\text{K}_2\text{HPO}_4/\text{H}_2\text{O/PEG}}^{(1)} = 1.51029 \times 10^{-2}$	5	0.068	41
BMIM-N(CF ₃ SO ₂) ₂ (IL ₁) + water ^a $t = 20-50$ °C	$\Gamma_{\text{BMIMNTf}_6/\text{H}_2\text{O/IL}_1}^0 = -1.25041$ $K_{\text{BMIMNTf}_6/\text{H}_2\text{O/IL}_1}^{(1)} = 5.28137 \times 10^{-2}$ $k_{\text{H}_2\text{O/IL}_1}^{(0)} = 0.1767265$ $k_{\text{H}_2\text{O/IL}_1}^{(1)} = 0.0186538$	7	0.051	40
EMIM-N(CF ₃ SO ₂) ₂ (IL ₂) + water ^a $t = 20-50$ °C	$\Gamma_{\text{EMIMNTf}_6/\text{H}_2\text{O/IL}_2}^0 = 2.87387$ $\Gamma_{\text{EMIMNTf}_6/\text{H}_2\text{O/IL}_2}^{(2)} = -1293.18$ $K_{\text{EMIMNTf}_6/\text{H}_2\text{O/IL}_2}^{(1)} = 1.64198 \times 10^{-2}$ $k_{\text{H}_2\text{O/IL}_2}^{(0)} = 0.0637980$ $k_{\text{H}_2\text{O/IL}_2}^{(1)} = 0.0931785$	7	0.029	40
EMIM-BE ₄ + water + <i>n</i> -hexane $t = 25$ °C, wt% _{EMIM-BE₄} = 0–100 in the aqueous phase	$\Gamma_{\text{BMIM-BE}_4/\text{H}_2\text{O/C}_6\text{H}_{14}}^0 = 6.13971 \times 10^{-3}$ $K_{\text{BMIM-BE}_4/\text{H}_2\text{O/C}_6\text{H}_{14}}^{(1)} = 35.7300$ $\Gamma_{\text{BMIM-BE}_4/\text{H}_2\text{O/C}_6\text{H}_{14}}^0 = 1.06440 \times 10^{-2}$ $K_{\text{BMIM-BE}_4/\text{H}_2\text{O/C}_6\text{H}_{14}}^{(1)} = 216.555$	8	0.357	49
BMIM-BE ₄ + water + <i>n</i> -hexane $t = 25$ °C, wt% _{BMIM-BE₄} = 0–100 in the aqueous phase	$\Gamma_{\text{BMIM-BE}_4/\text{H}_2\text{O/C}_6\text{H}_{14}}^0 = 9.13001 \times 10^{-2}$ $K_{\text{BMIM-BE}_4/\text{H}_2\text{O/C}_6\text{H}_{14}}^{(1)} = 1.07614$ $\Gamma_{\text{BMIM-BE}_4/\text{H}_2\text{O/C}_6\text{H}_{14}}^0 = -3.17001 \times 10^{-3}$ $K_{\text{BMIM-BE}_4/\text{H}_2\text{O/C}_6\text{H}_{14}}^{(1)} = 20.4053$	8	0.347	49

^a $k_{\text{H}_2\text{O/IL}} = k_{\text{IL,H}_2\text{O}}$ for these systems.

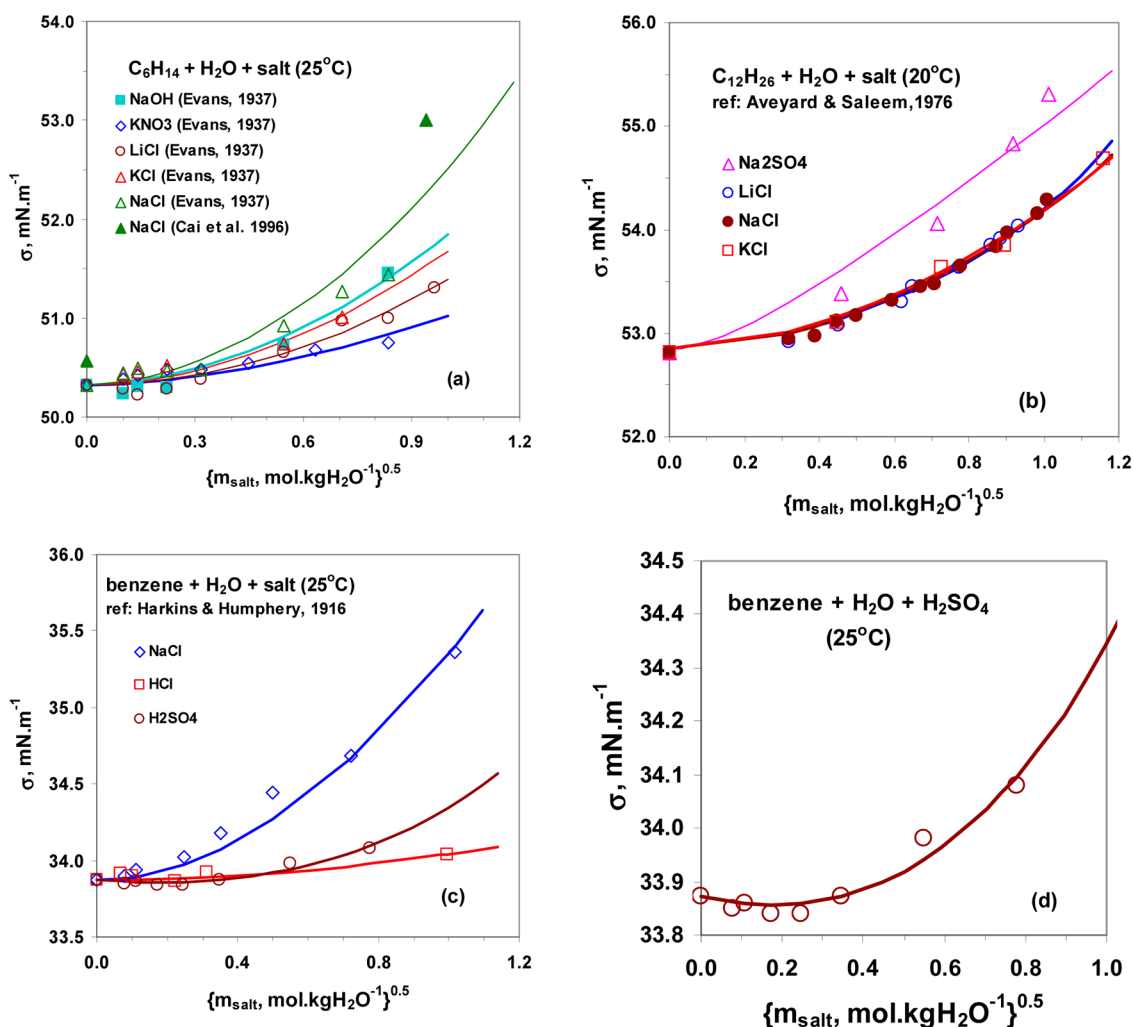


Figure 8. Variations of interfacial tension with the square root of electrolyte concentration ($m^{0.5}$) in (a) *n*-hexane + water + salt, (b) *n*-dodecane + water + salt, and (c) benzene + water + salt systems. The symbols denote literature data,^{42,43,45,48} and the lines were calculated using eqs 4–6 and 22. The results for the benzene + water + H₂SO₄ system in panel c are extended in panel d to show more detail.

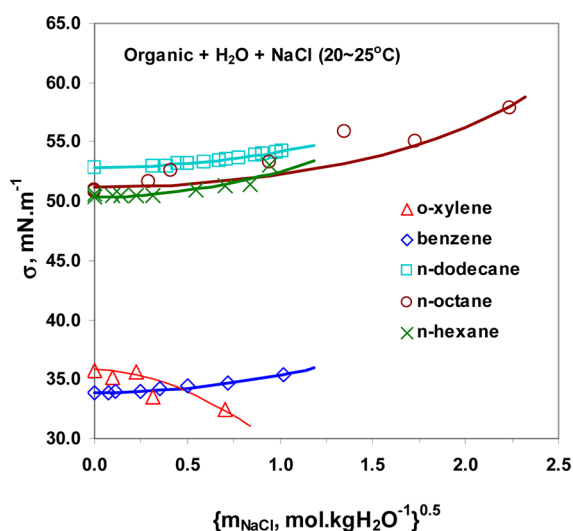


Figure 9. Variations of interfacial tension with the square root of NaCl concentration ($m^{0.5}$) in the aqueous phase of organic/aqueous NaCl systems. The symbols denote literature data,^{42,43,45–48} and the lines were calculated using eqs 4–6 and 22.

illustrated in Figure 11, good agreement with experimental data was obtained for the investigated ionic liquid + water systems over the temperature range from 20 to 50 °C.

In the two investigated ternary systems with ionic liquid components, EMIM·BF₄ + water + *n*-hexane and BMIM·BF₄ + water + *n*-hexane, both ionic liquids are miscible with water but immiscible with *n*-hexane.⁴⁹ These systems were treated in the same way as the organic + water + salt systems. Accordingly, the dissociated and undissociated ionic liquid components were treated as solutes, whereas water and *n*-hexane were defined as solvents. The interfacial tension in these two systems decreases significantly with the ionic liquid concentration at low IL contents and then levels off with a further increase in IL concentration. The decrease in the interfacial tension is more pronounced for the system with BMIM·BF₄, which also exhibits a dip at a mole fraction of 0.03 in the aqueous phase (cf. Figure 12). By calculating LLE from the thermodynamic model and introducing the $\Gamma_{ik}^{\sigma,0}$ and K_{ik} parameters for the {EMIM⁺, BF₄⁻} or {BMIM⁺, BF₄⁻} pairs and for the {EMIM·BF₄⁰, BF₄⁻} or {BMIM·BF₄⁰, BF₄⁻} pairs, the complex behavior of the interfacial tension in these two systems is accurately reproduced. The calculated interfacial tension is compared with experimental data in Figure 12, and excellent agreement can be observed.

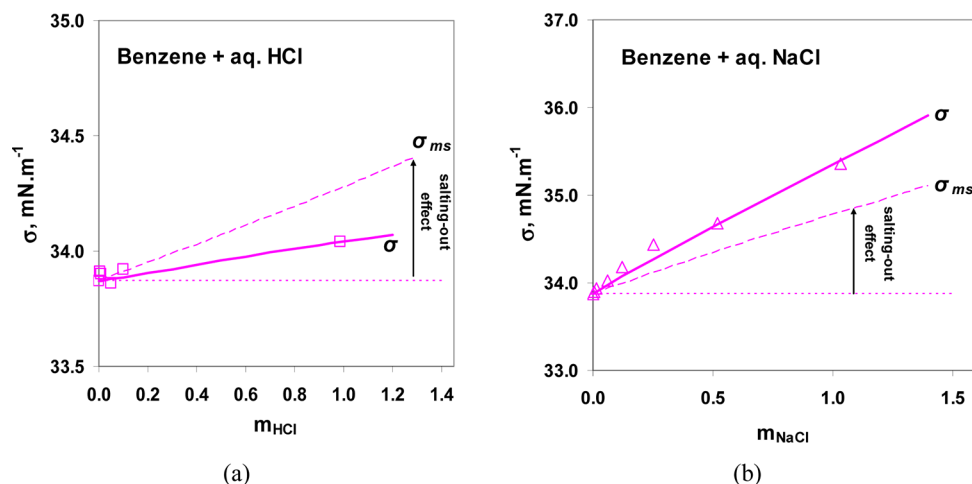


Figure 10. Variations of interfacial tension with electrolyte concentration (m) in the aqueous phase of organic/aqueous systems. The dashed lines were obtained from eqs 4–6 and 22 when the values of the ionic interaction parameters $\Gamma_i^{\sigma,0}$ and K_{ik} were both equal to 0, and the solid lines were calculated using regressed values of these parameters as listed in Table 4. The symbols denote literature data.⁴⁵

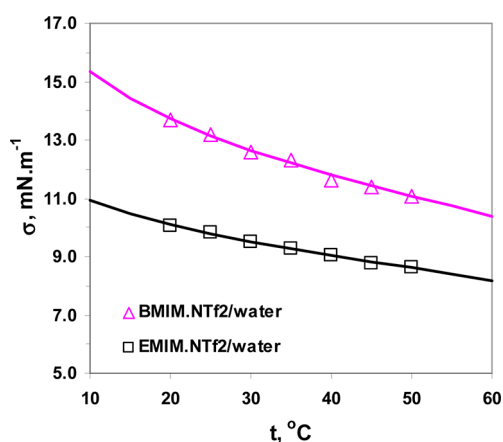


Figure 11. Interfacial tension along the liquid–liquid phase boundary in the BMIM·N(CF₃SO₂)₂ + water and EMIM·N(CF₃SO₂)₂ + water systems as a function of temperature. The symbols denote literature data,⁴⁰ and the lines were calculated using eqs 4–6 and 22.

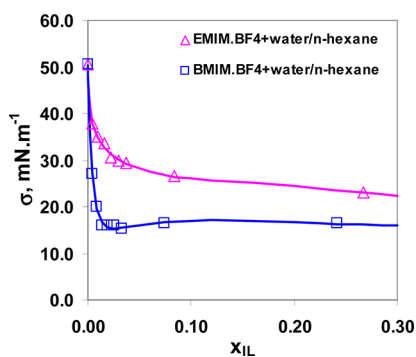


Figure 12. Interfacial tension along the liquid–liquid phase boundary in aqueous BMIM·BF₄ + *n*-hexane and aqueous EMIM·BF₄ + *n*-hexane systems as a function of the ionic liquid mole fractions in the aqueous phase. The symbols denote literature data,⁴⁹ and the lines were calculated using eqs 4–6 and 22.

The interfacial tension model was also applied to aqueous two-phase systems (ATPSs) containing a polymer and a salt. Such systems are an important class of mixtures used for separating and concentrating biomolecules. Interfacial tension

in these systems is important because it influences the partitioning behavior of the materials that are to be separated. In an ATPS, both immiscible phases are water-based. The polymer component in the ATPS phases is water-soluble and does not form two liquid phases with water without the presence of a salt. The interfacial tension model was tested for the ATPS systems composed of poly(ethylene glycol) (PEG) and a salt. Results of calculations for two such systems are given in Table 4. The interfacial tension data can be best reproduced when the binary ion parameters $\Gamma_{ik}^{\sigma,0}$ and K_{ik} are introduced between the prevailing cations and anions (e.g., K⁺/HPO₄^{2−} and NH₄⁺/SO₄^{2−}) in each system. Although no liquid–liquid base system exists for the ATPS, PEG and water are treated as solvent components in the interfacial tension model. However, no solvent interactions (i.e., $k_{\text{PEG,H}_2\text{O}}$) are introduced. It is noteworthy that the interfacial tension in such systems is very low (i.e., below 0.4 mN·m^{−1}) and is very sensitive to the accuracy of the calculated liquid–liquid equilibria. For example, an average deviation of only 0.068 mN·m^{−1} for the system PEG4000 + water + K₂HPO₄ corresponds to a relative error of 67%. An improved representation of liquid–liquid equilibria for such systems can enhance the accuracy of the calculated interfacial tension.

The interfacial tension model was also tested for liquid–liquid systems containing mixed electrolytes, although the available data for such systems are sparse. Table 4 lists the results for two quaternary systems: NaCl + CaCl₂ + water + *n*-hexane and NaCl + CaCl₂ + water + *n*-decane.⁴³ Both systems have only a limited number of data points at 25 and 50 °C at a single set of mixed electrolyte concentrations. The results for the system NaCl + CaCl₂ + water + *n*-hexane are shown in Figure 13. It is noteworthy that the interfacial tension in this system is represented well within the experimental uncertainty based only on the binary parameters $\Gamma_{ik}^{\sigma,0}$ and K_{ik} for {Na⁺, Cl[−]} and the predicted salting-out effects of CaCl₂. No binary parameters for {Ca²⁺, Cl[−]} were introduced.

6. CONCLUSIONS

A general model has been developed for calculating the interfacial tension of liquid–liquid systems with or without electrolyte components. The model consists of an equation for computing the interfacial tension of two-phase nonelectrolyte

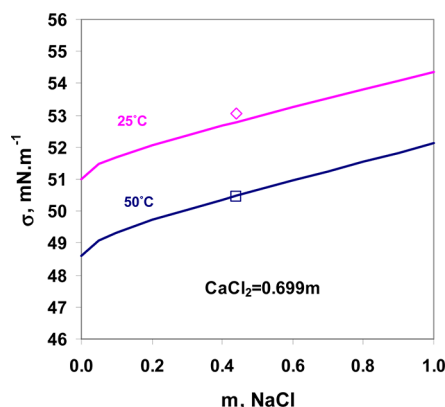


Figure 13. Predicted interfacial tension along the liquid–liquid phase boundary in the NaCl + CaCl₂ + water + *n*-hexane system as a function of the NaCl molality at a fixed CaCl₂ concentration ($m_{\text{CaCl}_2} = 0.699$) in water. The symbols denote literature data,⁴³ and the lines were calculated using eqs 4–6 and 22.

systems and an expression for the effect of electrolyte concentration. The expression for the interfacial tension of nonelectrolyte liquid–liquid systems was derived using a general thermodynamic framework, which was parametrized by introducing an effective interfacial area that is defined for each component and takes into account the interactions between different components at the interface. The dependence of interfacial tension on electrolyte concentration was derived from the Gibbs equation combined with a modified Langmuir adsorption isotherm that quantifies the interfacial excess of solute species. The model extends the Langmuir adsorption formalism by introducing the effects of binary interactions between solute species (ions or molecules) on the interface. The combined model was shown to reproduce experimental data for a variety of liquid–liquid systems. In particular, it accurately predicts the interfacial tension of ternary mixtures using parameters determined from only binary data. The coupling of the interfacial tension model with a previously developed thermodynamic model for equilibrium concentrations and activity coefficients makes it possible to reproduce the effects of complexation or other solution reactions on interfacial tension. For systems with electrolyte components, the model predicts reasonable trends of σ with electrolyte concentration using only bulk-phase thermodynamic input information without the need to introduce specific binary parameters for ions. This is an important advantage of the new model for predicting interfacial tension in the absence of experimental data. In all cases for which experimental data are available and have been tested, the new model was shown to reproduce interfacial tension over wide ranges of temperature and electrolyte concentration.

■ APPENDIX A. THERMODYNAMIC FRAMEWORK FOR INTERFACIAL TENSION IN NONELECTROLYTE LIQUID–LIQUID SYSTEMS

Following Shain and Prausnitz,¹ the derivation of the thermodynamic framework for interfacial tension starts from a definition of a fictitious chemical potential at the interface between the two liquid phases, α and β , so that a restriction of constant area does not appear. Accordingly

$$\mu_i^{\text{int}} \equiv \left(\frac{\partial G}{\partial N_i^{\text{int}}} \right)_{T, P, N_j^\alpha, N_j^\beta, N_k^{\text{int}} (k \neq i)} \quad (\text{A1})$$

where G is the Gibbs energy, T is the temperature, P is the pressure, N_i is the number of moles of component i , and the superscript int pertains to the interfacial region. Equation 1 can also be written as

$$\mu_i^{\text{int}} = \left(\frac{\partial G}{\partial N_i^{\text{int}}} \right)_{T, P, N_j^\alpha, N_j^\beta, N_k^{\text{int}} (k \neq i), A} + \left(\frac{\partial G}{\partial A} \right)_{T, P, N_j^\alpha, N_j^\beta, N_j^{\text{int}}} \left(\frac{\partial A}{\partial N_i^{\text{int}}} \right)_{T, P, N_j^\alpha, N_j^\beta, N_k^{\text{int}} (k \neq i)} \quad (\text{A1a})$$

where A is the interfacial area. From classical surface thermodynamics

$$\left(\frac{\partial G}{\partial N_i^{\text{int}}} \right)_{T, P, N_j^\alpha, N_j^\beta, N_k^{\text{int}} (k \neq i), A} = \mu_i \quad (\text{A2})$$

$$\left(\frac{\partial G}{\partial A} \right)_{T, P, N_j^\alpha, N_j^\beta, N_j^{\text{int}}} = \sigma \quad (\text{A3})$$

$$\left(\frac{\partial A}{\partial N_i^{\text{int}}} \right)_{T, P, N_j^\alpha, N_j^\beta, N_k^{\text{int}} (k \neq i)} = \overline{A_i^{\text{int}}} \quad (\text{A4})$$

where μ_i is the true chemical potential of component i and is related to the activity (a_i) in the liquid phase by

$$\mu_i = \mu_i^0 + RT \ln a_i \quad (\text{A5})$$

In eqs A3 and A4, σ is the interfacial tension, and $\overline{A_i^{\text{int}}}$ is the partial molar interfacial area of component i . Equations A1–A4 yield

$$\mu_i^{\text{int}} = \mu_i + \sigma \overline{A_i^{\text{int}}} \quad (\text{A6})$$

In analogy to eq A5 for bulk fluids, a fictitious interfacial activity, a_i^{int} , is defined as

$$\mu_i^{\text{int}} = \mu_i^{0, \text{int}} + RT \ln a_i^{\text{int}} \quad (\text{A7})$$

When the standard chemical potential in the interfacial phase is chosen to be the same as in the bulk liquid phase, that is, $\mu_i^{0, \text{int}} = \mu_i^0$, eq A7 becomes

$$\mu_i^{\text{int}} = \mu_i^0 + RT \ln a_i^{\text{int}} \quad (\text{A7a})$$

Equations A5–A7 lead to the following expression for the interfacial tension

$$\sigma = \frac{RT}{\overline{A_i^{\text{int}}}} \ln \left(\frac{a_i^{\text{int}}}{a_i} \right) \quad (\text{A8})$$

where $a_i \neq a_i^{\text{int}}$, $a_i = a_i^\alpha = a_i^\beta = x_i^\alpha \gamma_i^\alpha = x_i^\beta \gamma_i^\beta = x_i \gamma_i$, and $a_i^{\text{int}} = x_i^{\text{int}} \gamma_i^{\text{int}}$, and eq A8 becomes

$$\sigma = \frac{RT}{\overline{A_i^{\text{int}}}} \ln \left(\frac{x_i^{\text{int}} \gamma_i^{\text{int}}}{x_i \gamma_i} \right) \quad (\text{A8a})$$

or

$$x_i \gamma_i = x_i^{\text{int}} \gamma_i^{\text{int}} \exp \left(- \frac{\sigma A_i^{\text{int}}}{RT} \right) \quad (\text{A8b})$$

This equation, originally derived by Shain and Prausnitz,¹ provides a thermodynamic foundation for the model developed in this study.

AUTHOR INFORMATION

Corresponding Author

*E-mail: Pwang@olisystems.com. Tel.: 973-539-4996. Fax: 973-539-5922.

Notes

The authors declare no competing financial interest.

ACKNOWLEDGMENTS

The work reported herein was supported by Alcoa, Areva, ConocoPhillips, Dow Chemical, Mitsubishi Chemical, and Shell. The authors thank Adrian Ferramosca, Honggang Zhao, and Robert D. Young for their assistance in integrating the interfacial tension model with the thermodynamic framework in the OLI software. The authors also thank one of the reviewers for a constructive suggestion regarding the mixing rule for nonelectrolyte liquid–liquid systems.

REFERENCES

- (1) Shain, S. A.; Prausnitz, J. M. Thermodynamics and interfacial tension of multicomponent liquid–liquid interfaces. *AIChE J.* **1964**, *10* (5), 766–773.
- (2) Fu, J.; Li, B.; Wang, Z. Estimation of fluid–fluid interfacial tensions of multicomponent mixtures. *Chem. Eng. Sci.* **1986**, *41* (10), 2673–2679.
- (3) Li, B.; Fu, J. Quasi-lattice model of liquid–liquid interfacial tension for binary systems. *Fluid Phase Equilib.* **1991**, *64*, 129–139.
- (4) Li, B.; Fu, J. Estimation of interfacial tensions of ternary liquid–liquid systems by UNIQUAC method. *Fluid Phase Equilib.* **1992**, *81*, 129–152.
- (5) Donahue, D. J.; Bartell, F. E. The Boundary Tension at Water–Organic Liquid Interfaces. *J. Phys. Chem.* **1952**, *56*, 480–484.
- (6) Backes, H. M.; Ma, J. J.; Bender, E.; Maurer, G. Interfacial tensions in binary and ternary liquid–liquid systems. *Chem. Eng. Sci.* **1990**, *45* (1), 275–286.
- (7) Bahramian, A.; Danesh, A. Prediction of liquid–liquid interfacial tension in multi-component systems. *Fluid Phase Equilib.* **2004**, *221*, 197–205.
- (8) Bahramian, A. Mutual solubility–interfacial tension relationship in aqueous binary and ternary hydrocarbon systems. *Fluid Phase Equilib.* **2009**, *285*, 24–29.
- (9) Pliskin, I.; Treybal, R. E. Interfacial tensions of binary and ternary two-phase liquid systems. *AIChE J.* **1966**, *12* (4), 795–801.
- (10) Yarranton, H. W.; Masliyah, J. H. Gibbs–Langmuir Model for Interfacial Tension of Nonideal Organic Mixtures over Water. *J. Phys. Chem.* **1996**, *100* (5), 1786–1792.
- (11) Demond, A. H.; Lindner, A. S. Estimation of Interfacial Tension between Organic Liquids and Water. *Environ. Sci. Technol.* **1993**, *27*, 2318–2331.
- (12) Adamson, A. W.; Gast, A. P. *Physical Chemistry of Surfaces*, 6th ed.; John Wiley & Sons, Inc.: New York, 1997.
- (13) Girifalco, L. A.; Good, R. J. A Theory for the Estimation of Surface and Interfacial Energies. I. Derivation and Application to Interfacial Tension. *J. Phys. Chem.* **1957**, *61* (7), 904–909.
- (14) Cornelisse, P. M. W.; Wijkamp, M.; Peters, C. J.; de Swaan Arons, J. Interfacial tensions of fluid mixtures with polar and associating components. *Fluid Phase Equilib.* **1998**, *150–151*, 633–640.
- (15) Fleming, P. D.; Vinatieri, J. E.; Glinsmann, G. R. Theory of Interfacial Tensions in Multicomponent Systems. *J. Phys. Chem.* **1980**, *84* (12), 1526–1531.
- (16) Glinski, J. An empirical relation between mutual solubilities and interfacial tension for two partially miscible liquids. *Physica B* **1994**, *193*, 154–160.
- (17) Poling, B. E.; Prausnitz, J. M.; O'Connell, J. P. *The Properties of Gases and Liquids*, 5th ed.; McGraw-Hill: New York, 2001.
- (18) Yoon, H.; Oostrom, M.; Werth, C. J. Estimation of Interfacial Tension between Organic Liquid Mixtures and Water. *Environ. Sci. Technol.* **2009**, *43* (20), 7754–7761.
- (19) Volkov, A. G.; Deamer, D. W.; Tanelian, D. L.; Markin, V. S. Electrical double layers at the oil/water interface. *Prog. Surf. Sci.* **1996**, *53* (1), 1–134.
- (20) Bier, M.; Zwanikken, J.; van Roij, R. Liquid–liquid interfacial tension of electrolyte solutions. *Phys. Rev. Lett.* **2008**, *101* (4), 046104.
- (21) Onuki, A. Nonionic and ionic surfactants at an interface. *Europhys. Lett.* **2008**, *82*, 58002.
- (22) dos Santos, A. P.; Levin, Y. Surface and interfacial tensions of Hofmeister electrolytes. *Faraday Discuss.* **2012**, DOI: 10.1039/C2FD20067H.
- (23) dos Santos, A. P.; Levin, Y. Ions at the Water–Oil Interface: Interfacial Tension of Electrolyte Solutions. *Langmuir* **2012**, *28*, 1304–1308.
- (24) Onsager, L.; Samaras, N. N. T. The surface tension of Debye–Hückel electrolytes. *J. Chem. Phys.* **1934**, *2*, 528–536.
- (25) Desnoyer, C.; Masbernard, O.; Gourdon, C. Predictive model for the calculation of interfacial tension in nonideal electrolytic systems. *J. Colloid Interface Sci.* **1997**, *191*, 22–29.
- (26) Li, Z.; Lu, B. C.-Y. Prediction of Interfacial Tension between an Organic Solvent and Aqueous Solutions of Mixed Electrolytes. *Fluid Phase Equilib.* **2002**, *200*, 239–250.
- (27) Meissner, H. P.; Newman, S. A. Prediction of activity coefficients of strong electrolytes in aqueous systems. *ACS Symp. Ser.* **1980**, *133*, 495–511.
- (28) Wang, P.; Anderko, A.; Young, R. D. A speciation-based model for mixed-solvent electrolyte systems. *Fluid Phase Equilib.* **2002**, *203* (1–2), 141–176.
- (29) Sprow, F. B.; Prausnitz, J. M. Surface tension of simple liquid mixtures. *Trans. Faraday Soc.* **1966**, *62*, 1105–1111.
- (30) Bondi, A. A. *Physical Properties of Molecular Crystals, Liquids, and Glasses*; John Wiley and Sons: New York, 1968.
- (31) Abrams, D. S.; Prausnitz, J. M. Statistical thermodynamics of liquid mixtures: New expressions for excess Gibbs energy of partly or completely miscible systems. *AIChE J.* **1975**, *21* (1), 116–128.
- (32) Michelsen, M. L.; Kistenmacher, H. On composition-dependent interaction coefficients. *Fluid Phase Equilib.* **1990**, *58*, 229–230.
- (33) Wang, P.; Anderko, A.; Springer, R. D.; Young, R. D. Modeling phase equilibria and speciation in mixed-solvent electrolyte systems: II. Liquid–liquid equilibria and properties of associating electrolyte solutions. *J. Mol. Liq.* **2006**, *125* (1), 37–44.
- (34) Wang, P.; Anderko, A. Modeling chemical equilibria, phase behavior, and transport properties in ionic liquid systems. *Fluid Phase Equilib.* **2011**, *302* (1–2), 74–82.
- (35) Guggenheim, E. A.; Adam, N. K. The Thermodynamics of Adsorption at the Surface of Solutions. *Proc. R. Soc. London A* **1933**, *139* (837), 218–236.
- (36) Haynes, C. A.; Carson, J.; Blanch, H. W.; Prausnitz, J. M. Electrostatic potentials and protein partitioning in aqueous two-phase systems. *AIChE J.* **1991**, *37* (9), 1401–1409.
- (37) Wang, P.; Anderko, A.; Young, R. D. Modeling surface tension of concentrated and mixed-solvent electrolyte systems. *Ind. Eng. Chem. Res.* **2011**, *50* (7), 4086–4098.
- (38) Li, Z. B.; Lu, B. C. Y. Surface tension of aqueous electrolyte solutions at high concentrations—Representation and prediction. *Chem. Eng. Sci.* **2001**, *56* (8), 2879–2888.
- (39) Damaskin, B. B.; Petrii, O. A.; Batrakov, V. V. *Adsorption of Organic Compounds on Electrodes*; Plenum Press: New York, 1971.

- (40) Gardas, R. L.; Ge, R.; Manan, N. A.; Rooney, D. W.; Hardacre, C. Interfacial tensions of inidazolium-based ionic liquids with water and *n*-alkanes. *Fluid Phase Equilib.* **2010**, *294*, 139–147.
- (41) Wu, Y.-T.; Zhu, Z.-Q.; Mei, L.-H. Interfacial Tension of Poly(ethylene glycol) + Salt + Water Systems. *J. Chem. Eng. Data* **1996**, *41* (5), 1032–1035.
- (42) Aveyard, R.; Saleem, S. M. Interfacial tensions at alkane–aqueous electrolyte interfaces. *J. Chem. Soc., Faraday Trans. 1* **1976**, *72*, 1609–1617.
- (43) Cai, B.-Y.; Yang, J.-T.; Guo, T.-M. Interfacial Tension of Hydrocarbon + Water/Brine Systems under High Pressure. *J. Chem. Eng. Data* **1996**, *41* (3), 493–496.
- (44) Guest, W. L.; Lewis, W. C. M. The effect of electrolytes upon the interfacial tension between water and dekaline (*trans*-decahydronaphthalene). *Proc. R. Soc. London A* **1939**, *170* (943), 501–513.
- (45) Harkins, W. D.; Humphrey, E. C. The Surface Tension at the Interface between Two Liquids, and the Effect of Acids, Salts and Bases upon the Interfacial Tension. *J. Am. Chem. Soc.* **1916**, *38* (2), 242–246.
- (46) Dussaud, A.; Vignes-Adler, M. Wetting Transition of *n*-Alkanes on Concentrated Aqueous Salt Solutions. Line Tension Effect. *Langmuir* **1997**, *13* (3), 581–589.
- (47) Lord, D. L.; Hayes, K. F.; Demond, A. H.; Salehzadeh, A. Influence of Organic Acid Solution Chemistry on Subsurface Transport Properties. I. Surface and Interfacial Tension. *Environ. Sci. Technol.* **1997**, *31* (7), 2045–2051.
- (48) Evans, A. W. The effect of uni-univalent electrolytes upon the interfacial tension between *n*-hexane and water. *Trans. Faraday Soc.* **1937**, *33*, 794–800.
- (49) Zhu, L. Applications of room temperature ionic liquids in interfacial polymerization. Ph.D. Thesis, New Jersey Institute of Technology, Newark, NJ, 2006.
- (50) Zuidema, H. H.; Pilz, G. P. Interfacial Tension between Water and Organic Liquids Heavier than Water. *Anal. Chem.* **1948**, *20* (12), 1244–1245.
- (51) Pliskin, I.; Treybal, R. E. Interfacial Tension in Two-Liquid-Phase Ternary Systems. *J. Chem. Eng. Data* **1966**, *11* (1), 49–52.
- (52) Sada, E.; Kito, S.; Yamashita, M. Interfacial Tensions of Two-Phase Ternary Systems. *J. Chem. Eng. Data* **1975**, *20* (4), 376–377.
- (53) Paul, G. W.; Marc de Chazal, L. E. Interfacial Tensions in Ternary Liquid–Liquid Systems. *J. Chem. Eng. Data* **1967**, *12* (1), 105–107.
- (54) Rose, S.; Patterson, R. E. Surface and Interfacial Tensions of Conjugate Solutions in Ternary Systems. *J. Chem. Eng. Data* **1979**, *24* (2), 111–115.
- (55) Frenkel, M.; Chirico, R. D.; Diky, V.; Muzny, C. D.; Kazakov, A. F.; Magee, J. W.; Abdulgatov, I. M.; Kroenlein, K.; Kang, J. W. *ThermoData Engine (TDE) Version 6.0—Pure Compounds, Binary Mixtures, Ternary Mixtures, and Chemical Reactions*; Standard Reference Database 103b; National Institute of Standards and Technology: Gaithersburg, MD, 2011.
- (56) Chavepeyer, G.; Platten, J. K.; Ouazzani, M. T.; Gliniski, J.; Cornu, D. Interfacial tension data analysis of partially miscible binary organic–organic or organic–water systems near a critical consolute temperature. *J. Colloid Interface Sci.* **1993**, *157*, 278–284.
- (57) Schreinemakers, F. A. H. Vapor pressures in the system: Water, acetone and phenol. I. *Z. Phys. Chem.* **1902**, *39* (4), 485–510.
- (58) Hill, A. E.; Malisoff, W. M. The Mutual Solubility of Liquids. III. The Mutual Solubility of Phenol and Water. IV. The Mutual Solubility of Normal Butyl Alcohol and Water. *J. Am. Chem. Soc.* **1926**, *48* (4), 918–927.
- (59) Campbell, A. N.; Campbell, A. J. R. Concentrations, Total and Partial Vapor Pressures, Surface Tensions and Viscosities in the Systems Phenol–Water and Phenol–Water–4% Succinic Acid. *J. Am. Chem. Soc.* **1937**, *59* (12), 2481–2488.
- (60) Jones, E. R. Some Observations on the System Phenol–Water. *J. Phys. Chem.* **1927**, *31* (9), 1316–1321.
- (61) Campbell, A. N. The System Aniline–Phenol–Water. *J. Am. Chem. Soc.* **1945**, *67* (6), 981–987.
- (62) Lyzlova, R. V.; Susarev, M. P. Phase Equilibria in the Water–Hydrogen Chloride–Phenol Ternary System. *Russ. J. Appl. Chem.* **1982**, *55* (2), 233–236.
- (63) Stephenson, R. M. Mutual Solubility of Water and Aliphatic Amines. *J. Chem. Eng. Data* **1993**, *38* (4), 625–629.
- (64) De Santis, R. Phase Equilibria of the Water + Sodium Chloride + Triethylamine System. *J. Chem. Eng. Data* **1976**, *21* (3), 328–330.
- (65) Davidson, R. R.; Smith, W. H.; Hood, D. W. Structure and Amine–Water Solubility in Desalination by Solvent Extraction. *J. Chem. Eng. Data* **1960**, *5* (4), 420–423.
- (66) Villers, D.; Platten, J. K. Temperature Dependence of the Interfacial Tension between Water and Long-Chain Alcohols. *J. Phys. Chem.* **1988**, *92* (14), 4023–4024.
- (67) Saïen, J.; Salimi, A. Interfacial Tension of Saturated Butan-1-ol + Sodium Dodecyl Sulfate + Saturated Water from 20 to 50 °C and pH between 4 and 9. *J. Chem. Eng. Data* **2004**, *49* (4), 933–936.
- (68) Heertjes, P. M.; de Smet, E. C.; Witvoet, W. C. The determination of interfacial tensions with the Wilhelmy plate method. *Chem. Eng. Sci.* **1971**, *26*, 1479–1480.
- (69) Xu, J. H.; Li, S. W.; Lan, W. J.; Luo, G. S. Microfluid Approach for Rapid Interfacial Tension Measurement. *Langmuir* **2008**, *24* (19), 11287–11292.
- (70) Prochazka, O.; Suska, J.; Pick, J. Phase equilibria in the methanol + water + 1-butanol system. *Collect. Czech. Chem. Commun.* **1975**, *40*, 781–786.
- (71) Reber, L. A.; McNabb, W. M.; Lucasse, W. W. The Effect of Salts on the Mutual Miscibility of Normal Butyl Alcohol and Water. *J. Phys. Chem.* **1942**, *46* (4), 500–515.
- (72) Drouillon, F. Study of the ternary mixture water–ethyl alcohol–normal butyl alcohol. *J. Chim. Phys. Phys. Chim. Biol.* **1925**, *22*, 149–160.
- (73) Jones, D. C. The systems *n*-butyl alcohol–water and *n*-butyl alcohol–acetone–water. *J. Chem. Soc.* **1929**, 799–813.
- (74) Aoki, Y.; Moriyoshi, T. Mutual solubility of *n*-butanol + water under high pressures. *J. Chem. Thermodyn.* **1978**, *10* (12), 1173–1179.
- (75) Mori, Y. H.; Tsui, N.; Kiyomiya, M. Surface and Interfacial Tensions and Their Combined Properties in Seven Binary, Immiscible Liquid–Liquid–Vapor Systems. *J. Chem. Eng. Data* **1984**, *29* (4), 407–412.
- (76) Matsubara, H.; Murase, M.; Mori, Y. H.; Nagashima, A. Measurement of the surface tensions and the interfacial tensions of *n*-pentane–water and R113–water systems. *Int. J. Thermophys.* **1988**, *9* (3), 409–424.
- (77) Pomerantz, P.; Clinton, W. C.; Zisman, W. A. Spreading pressures and coefficients, interfacial tensions and adhesion energies of the alkanes, alkenes, and alkyl benzenes on water. *J. Colloid Interface Sci.* **1967**, *24*, 16–28.
- (78) Johnson, R. E.; Dettre, R. H. The wettability of low-energy liquid surfaces. *J. Colloid Interface Sci.* **1966**, *21*, 610–622.
- (79) Goebel, A.; Lunkenheimer, K. Interfacial Tension of the Water/*n*-Alkane Interface. *Langmuir* **1997**, *13* (2), 369–372.
- (80) Zeppieri, S.; Rodriguez, J.; Lopez de Ramos, A. L. Interfacial Tension of Alkane + Water Systems. *J. Chem. Eng. Data* **2001**, *46* (5), 1086–1088.
- (81) Contreras, P.; Olteanu, M. Interfacial tension measurement by the rotating meniscus. *Colloids Surf. A* **2000**, *170*, 45–50.
- (82) Jańczuk, B.; Wójcik, W.; Zdziennicka, A. Determination of the components of the surface tension of some liquids from interfacial liquid–liquid tension measurements. *J. Colloid Interface Sci.* **1993**, *157*, 384–393.
- (83) Mitrinovic, D. M.; Tikhonov, A. M.; Li, M.; Huang, Z.; Schlossman, M. L. Noncapillary-wave structure at the water–alkane interface. *Phys. Rev. Lett.* **2000**, *85* (3), 582–585.
- (84) Liggieri, L.; Ravera, F.; Passerone, A. Equilibrium interfacial tension of hexane/water plus Triton X-100. *J. Colloid Interface Sci.* **1995**, *169*, 238–240.
- (85) Michaels, A. S.; Hauser, E. A. Interfacial tension at elevated pressure and temperature. II. Interfacial properties of hydrocarbon–water systems. *J. Phys. Colloid Chem.* **1951**, *55* (3), 408–421.

- (86) Jennings, H. Y. The Effect of Temperature and Pressure on the Interfacial Tension of Benzene–Water and *n*-Decane–Water. *J. Colloid Interface Sci.* **1967**, *24*, 323–329.
- (87) Rose, W. E.; Seyer, W. F. The Interfacial Tension of Some Hydrocarbons against Water. *J. Phys. Colloid Chem.* **1951**, *55* (3), 439–447.
- (88) Lofgren, H.; Neuman, R. D.; Scriven, L. E.; Davis, H. T. Laser light-scattering measurements of interfacial tension using optical heterodyne mixing spectroscopy. *J. Colloid Interface Sci.* **1984**, *98* (1), 175–183.
- (89) Jones, M. N. Interfacial tension studies at the aqueous urea–*n*-decane and aqueous urea + surfactant–*n*-decane interfaces. *J. Colloid Interface Sci.* **1973**, *44* (1), 13–19.
- (90) Inaba, H.; Sato, K. A measurement of interfacial tension between tetradecane and ethylene glycol water solution by means of the pendant drop method. *Fluid Phase Equilib.* **1996**, *125*, 159–168.
- (91) Matthews, J. B. Influence of certain carbohydrate substances upon the interfacial tension between water and cyclohexane. *Trans. Faraday Soc.* **1939**, *35*, 1113–1122.
- (92) Motomura, K.; Iyota, H.; Ikeda, N.; Aratono, M. Thermodynamic studies on adsorption at interface: VI. Interface between cyclohexane–benzene mixture and water. *J. Colloid Interface Sci.* **1988**, *126* (1), 26–36.
- (93) Cupples, H. L. Interfacial Tension by the Ring Method: The Benzene–Water Interface. *J. Phys. Colloid Chem.* **1947**, *51* (6), 1341–1345.
- (94) Harvey, R. R. The Effect of Pressure on the Interfacial Tension of Benzene–Water System. *J. Phys. Chem.* **1958**, *62*, 322–324.
- (95) Bartell, F. E.; Miller, F. L. A Method for the Measurement of Interfacial Tension of Liquid–Liquid Systems. *J. Am. Chem. Soc.* **1928**, *50*, 1961–1967.
- (96) Saien, J.; Akbari, S. Interfacial Tension of Toluene + Water + Sodium Dodecyl Sulfate from 20 to 50 °C and pH between 4 and 9. *J. Chem. Eng. Data* **2006**, *51* (5), 1832–1835.
- (97) Jasper, J. J.; Seitz, H. R. The Temperature–Interfacial Tension Studies of Some Alkylbenzenes against Water. *J. Phys. Chem.* **1959**, *63* (9), 1429–1431.
- (98) Chavepeyer, G.; De Saedeleer, C.; Platten, J. K. Temperature dependence of interfacial tension between normal organic acids and water. *J. Colloid Interface Sci.* **1994**, *167*, 464–466.
- (99) Costa, H. F.; Lourenco, H.; Johnson, I.; Goncalves, F. A. M. M.; Ferreira, A. G. M. Liquid–Liquid Equilibria, Density, Viscosity, and Surface and Interfacial Tension of the System Water + *n*-Butyl Acetate + 1-Propanol at 323 K and Atmospheric Pressure. *J. Chem. Eng. Data* **2009**, *54* (10), 2845–2854.
- (100) Al-Wahaibi, Y. M.; Grattoni, C. A.; Muggeridge, A. H. Physical Properties (Density, Viscosity, Surface Tension, Interfacial Tension, and Contact Angle) of the System Isopropyl Alcohol + Cyclohexane + Water. *J. Chem. Eng. Data* **2007**, *52* (2), 548–552.